PHYSICAL REVIEW D **90,** 123538 (2014)

Loop quantum cosmology of a radiation-dominated flat FLRW universe

Tomasz Pawłowski,[1,2,*] Roberto Pierini,[3,4,5,6,†] and Edward Wilson-Ewing[3,4,7,‡]

[1]*Departamento de Ciencias Físicas, Facultad de Ciencias Exactas, Universidad Andres Bello, Avenida República 220, Santiago 8370134, Chile*

[2]*Wydział Fizyki, Uniwersytet Warszawski, Hoża 69, 00-681 Warszawa, Poland*

[3]*Aix Marseille Université, CNRS, CPT, UMR 7332, 13288 Marseille, France*

[4]*Université de Toulon, CNRS, CPT, UMR 7332, 83957 La Garde, France*

[5]*School of Science and Technology, University of Camerino, I-62032 Camerino, Macerata, Italy*

[6]*INFN Sezione di Perugia, 06123 Perugia, Italy*

[7]*Department of Physics & Astronomy, Louisiana State University, Baton Rouge, Louisiana 70803-4001, USA*

(Received 23 April 2014; published 29 December 2014)

We study the loop quantum cosmology of a flat Friedmann-Lemaître-Robertson-Walker space-time with a Maxwell field. We show that many of the qualitative properties derived for the case of a massless scalar field also hold for a Maxwell field. In particular, the big-bang singularity is replaced by a quantum bounce, and the operator corresponding to the matter energy density is bounded above by the same critical energy density. We also numerically study the evolution of wave functions that are sharply peaked in the low energy regime, and derive effective equations which very closely approximate the full quantum dynamics of sharply peaked states at all times, including the near-bounce epoch. In the process, the analytical and numerical methods originally used to study the dynamics in loop quantum cosmology for the case of a massless scalar field are substantially improved to handle the difficulties (that generically arise for matter content other than a massless scalar field) related to the presence of a Maxwell field.

DOI: 10.1103/PhysRevD.90.123538 PACS numbers: 98.80.Qc, 04.60.Pp

I. INTRODUCTION

In loop quantum cosmology (LQC) [1], cosmological models are quantized in a nonperturbative manner using the basic operators and following the methods of loop quantum gravity (LQG). The first cosmologies to be studied were the homogeneous and isotropic Friedmann-Lemaître-Robertson-Walker (FLRW) space-times with a massless scalar field, where it was initially shown that the quantum equations of motion do not break down at the big-bang singularity [2], and then that the singularity is replaced by a quantum gravity "bounce" that connects a pre-bounce contracting FLRW space-time to a post-bounce expanding FLRW space-time [3,4].

These results have since been generalized to include FLRW space-times that allow nonzero spatial curvature [5,6], a nonzero cosmological constant [7] or have pressureless dust as the matter content [8] (the latter as a test for the full LQG framework proposed in [9] where an irrotational pressureless dust field acts as a clock[1]). In all of these cases the big-bang singularity has also been shown to be replaced by a bounce. Space-times that allow anisotropies [11–13] and inhomogeneities (using a hybrid quantization procedure) [14,15] have also been studied in LQC; in the Bianchi and Gowdy models, the classical singularity is resolved as the singular states decouple from the nonsingular states under the quantum dynamics. It is generally expected that the big-bang singularity is replaced by a bounce in this setting as well (see, e.g., studies of the effective equations for the LQC of the Bianchi I [16] and Gowdy [17] space-times), but this has not yet been shown as the full quantum dynamics have not yet been investigated. Indeed, dynamical studies of inhomogeneous cosmologies in LQC rely strongly on the extrapolation of the properties of systems studied at a genuinely quantum level, in particular the preservation of semiclassicality and the validity of the semiclassical effective dynamics as a good approximation to the quantum dynamics.

Most recently cosmological perturbations have also been studied in LQC, first from an effective theory standpoint [18] and then in quantum treatments following various approaches: a "hybrid" quantization (i.e., the LQC of the homogeneous background and a Fock quantization of the perturbative degrees of freedom) [19] (see also [20]) and by the LQC treatment of a discretization of the flat FLRW space-time with scalar perturbations [21]. These works have allowed the study of the dynamics of cosmological perturbations in the Planck regime in some of the most interesting cosmological scenarios—those that generate a scale-invariant power spectrum of scalar

*tomasz.pawlowski@unab.cl
†roberto.pierini@unicam.it
‡wilson-ewing@phys.lsu.edu

[1]The deparametrization of general relativity with respect to the irrotational dust field leads to a formulation of LQG with a true Hamiltonian for the gravitational and nondust matter degrees of freedom, and circumvents a series of technical obstacles in completing the quantization program. See also [10].

perturbations—namely inflation [22], the matter bounce [23] and the ekpyrotic universe [24].

In LQC, the main research effort is focused on investigating the loop quantum geometry effects, arising from a quantization which differs from the standard Wheeler-DeWitt one. The matter sector is usually dealt with in a perfunctory manner, although there do exist some studies on the polymeric matter sector in the literature [25,26] (including attempts to describe the perturbative degrees of freedom [27]). Most of the space-times studied to date in LQC are either vacuum space-times [12,14] or with the particularly simple choice of a massless scalar field [3,5–7,11,13,15]. While the cases of a massive scalar field in a flat FLRW space-time [28], and a vector field in the Bianchi I cosmology [29] have also been studied, a robust analysis of the dynamical sector of the theories at a genuinely quantum level has only been performed for matter choices (namely a massless scalar field or pressure-less dust) which are idealizations of realistic (from the point of view of particle physics) matter fields. In particular, the principal components of the standard model have never been systematically analyzed in this context and the LQC studies involving them rely on extrapolations from the above-mentioned idealizations. In the general context of cosmology, a particularly important case is a perfect fluid of radiation formed by standard model particles. This article is dedicated to the study of a radiation-dominated space-time in LQC in the most simple setting possible: by emulating a radiation-dominated perfect fluid with as few as possible homogeneous standard model matter fields.

As the resolution of cosmological singularities in LQC is due to the loop quantization of the gravitational sector (rather than any effect due to the matter fields), it seems reasonable to assume that the specific type of matter field does not affect the qualitative results of LQC and that the big-bang singularity is generically replaced by a quantum gravity bounce, regardless of the matter field. However, despite this expectation it is important to study a variety of matter fields in order to show that the results obtained for massless scalar fields do in fact hold more generally, especially in the situation when distinct fields are used as the emergent time (i.e., the fields are used as evolution parameters labeling the families of partial observables [30]), since the use of matter clocks has been essential in studies of the quantum dynamics to date.[2]

Another reason to study different matter fields is that it is not immediately obvious how to include some types of matter fields—e.g., vector fields—in minisuperspace models that assume homogeneity and isotropy. This is a tricky problem as a homogeneous vector field necessarily picks out a preferred direction, which is clearly at odds with isotropy. We show that a model earlier proposed in classical cosmology is suitable for the Hamiltonian framework, and thus for canonical quantum cosmology theories such as LQC.

Finally, concerning the matter content, the massless scalar field mostly used so far in the literature possesses a series of convenient properties that simplify the analysis. As we will see later in this paper (Secs. III and IV and Appendices A and B) other (more realistic) matter fields do not possess many of these properties. This makes the study of other fields significantly more difficult and in particular requires substantial revisions and extensions of the analytical and numerical methods used in previous studies, for example [3]. The increase in difficulty observed here for Maxwell fields is expected to be generic for standard model matter fields. Thus, the improvements to the methodology presented here may be essential for many further developments in LQC.

As a first step in addressing these issues, we will study the loop quantization of a flat FLRW space-time with a Maxwell field, the massless vector field that satisfies Maxwell's equations. This is a particularly interesting matter field for two reasons. First, it is a vector field, and therefore it will be necessary to determine how a vector field can be handled in a homogeneous and isotropic background. Second, the equation of state of a Maxwell field is that of radiation, namely $P = \rho/3$, where ρ is the energy density and P the pressure of the Maxwell field.

This second condition is particularly important as all matter fields with the dispersion relation $E = \sqrt{p^2 + m^2}$ that are in either the Bose-Einstein or Fermi-Dirac distribution behave like radiation at sufficiently high temperatures, that is they have the same equation of state $P \cong \rho/3$. As the two properties of the matter fields that enter into the Einstein equations in the homogeneous and isotropic limit are precisely their energy density and pressure, different fields that have the same initial ρ and the same equation of state lead to the same gravitational dynamics of the FLRW space-time. Therefore, at high temperatures (like the temperatures reached in the very early universe), all (of the populations) of the bosonic or fermionic fields that can be treated in a statistical manner are accurately mimicked by a population of Maxwell fields. Thus, the study of the Maxwell field in loop quantum cosmology is of wide interest, as it can provide a good approximation to many different types of thermalized matter fields in the Planck regime.

In this paper, following the improved dynamics loop quantization prescription [3], we will study in detail the quantum dynamics of the isotropic universe with a suitable population of Maxwell fields as matter content and in particular show that the big-bang singularity is replaced by a quantum bounce in LQC. This strongly suggests that the

[2]Once a particular matter field has been chosen as the internal clock, it is easy to generalize the presence of the bounce and the energy density boundedness results to the case of generic matter fields *added on top of* the clock fields. This is a direct consequence of the boundedness of the gravitational energy density operator (see for example the discussion in [8]).

initial cosmological singularity is resolved by quantum gravity effects in all flat FLRW space-times where the matter field at high temperatures is well approximated by radiation.

The outline of the paper is as follows. In Sec. II, the classical theory will be reviewed and in particular it will be shown how, following [31], a matter sector constituted of Maxwell fields can be made to be homogeneous and isotropic. Then in Sec. III the quantum theory will be defined and numerically solved for semiclassical states; some results concerning the asymptotic dynamics are presented in Sec. IV. The effective equations are presented in Sec. V, and we close with a discussion in Sec. VI. The technical derivations leading to the results presented in Sec. IV are contained in Appendices A and B.

The units we use in this paper are such that $c = 1$, but G and $\hbar$ will remain explicit; we define the Planck length as $\ell_{\mathrm{Pl}} = \sqrt{G\hbar}$. Greek letters μ, ν, ρ, σ represent space-time indices, while the roman letters at the beginning of the alphabet a, b, c represent spatial indices and i, j, k, l represent internal spatial indices.

II. VECTOR FIELDS IN ISOTROPIC COSMOLOGY

In this section, we shall review a simple model that allows vector fields to be included in homogeneous and isotropic minisuperspace models. The key point is that in a gas of photons, there are many individual photons evenly spread out over space (ensuring approximate homogeneity) which are traveling in all directions (ensuring approximate isotropy). In the statistical limit of a large number density of photons, the photon gas is homogeneous and isotropic.

One way to model the stress-energy tensor for a photon gas is by working with a linear combination of plane waves. In order to see this, recall that the stress-energy tensor for a single plane wave of radiation with amplitude A and (null) tangent 4-vector k^μ is

$$T_{\mu\nu} = \frac{A^2}{8\pi G} k_\mu k_\nu, \tag{2.1}$$

where we assume that we are interested in $T_{\mu\nu}$ only at scales larger than the wavelength of the plane wave [32].

In order to satisfy the isotropy requirement, it is necessary to have plane waves (with the same amplitude) traveling in all directions, and then

$$T_{\mu\nu} = \frac{A^2}{8\pi G} \int \mathrm{d}\theta \mathrm{d}\phi \sin\theta k_\mu(\theta,\phi) k_\nu(\theta,\phi), \tag{2.2}$$

where $k^\mu(\theta,\phi)$ is the tangent 4-vector of the plane wave traveling in the (θ,ϕ) direction on the FLRW space-time with the metric

$$\mathrm{d}s^2 = -N^2\mathrm{d}t^2 + a(t)^2 \mathrm{d}\vec{x}^2. \tag{2.3}$$

From this, it is easy to check that

$$T_{\mu\nu} = \rho u_\mu u_\nu + P(g_{\mu\nu} + u_\mu u_\nu), \tag{2.4}$$

with

$$\rho = \frac{A^2}{2G}, \qquad P = \frac{\rho}{3}, \tag{2.5}$$

and u^μ is the usual comoving 4-vector of the perfect fluid.

This shows how it is possible to model a perfect fluid of radiation as a linear combination of plane waves traveling in all directions. However, this setup is unwieldy in the Hamiltonian framework, so we will now introduce a toy model that gives the stress-energy tensor (2.4). In this toy model, there are three "species" or "flavors" of a Maxwell field [31] in a flat FLRW universe. This simpler setting is relatively easy to handle in a Hamiltonian setting, and so is more convenient for the quantum theory. In the following part, we describe this toy model, define the Hamiltonian for the matter and gravitational sectors, and conclude the section by briefly discussing the classical dynamics.

A. The three $U(1)$ vector fields

Motivated by the fact that a linear superposition of plane waves can yield a homogeneous and isotropic matter field, in this paper we will consider a particularly simple linear superposition of this type. To be specific, we take a linear superposition of three plane waves that are orthogonal and of equal amplitude. Furthermore, for simplicity we assume the wave number of these plane waves to be zero, which then each correspond to homogeneous field configurations. This particularly simple linear superposition of plane waves is a toy model of (2.2) which will make calculations in a canonical quantum framework tractable and allow us to define the loop quantum cosmology of a radiation-dominated space-time. While a more realistic model of a radiation-dominated space-time would be to consider a more general linear superposition of plane waves, this is very difficult to handle in a minisuperspace model of quantum cosmology and we leave this possibility for future work. Nonetheless, (2.2) does suggest using a simpler model—namely, the linear superposition of the three homogeneous (i.e., plane waves with zero momentum) and orthogonal vector fields—in order to study a radiation-dominated space-time.[3] This is what we

[3]Note that this simpler model remains very interesting as it does in fact capture the salient details of (2.2). This is because the wave number does not affect the gravitational dynamics since the energy density (as well as the pressure) contribution due to a plane wave is homogeneous and only depends on the amplitude of the plane wave as can be seen explicitly in (2.5). Thus, the restriction to one wave number will not affect the resulting physics insofar as the dynamics of the space-time are concerned (where only energy density and pressure enter into the Friedmann equations), and neither will the specific choice of setting the wave number to zero in order to obtain homogeneous solutions.

shall do in this paper, and in the remainder of this section we shall precisely define the model.

Denoting the vector potential of each field by $({}^{\alpha}A)_{\mu}$, where the index $\alpha = 1, 2, 3$ labels the three different $U(1)$ fields, the Lagrangian density for each of the three fields is given by

$$ {}^{\alpha}\mathcal{L} = -\frac{1}{4}\sqrt{-g}({}^{\alpha}F)_{\mu\nu}({}^{\alpha}F)^{\mu\nu}, \tag{2.6} $$

where $({}^{\alpha}F)_{\mu\nu}$ is the field strength of the vector field, $({}^{\alpha}F)_{\mu\nu} = 2\partial_{[\mu}({}^{\alpha}A)_{\nu]}$.

Now, in order to ensure the homogeneity and isotropy of the matter field, it is necessary to carefully choose the form of the $({}^{\alpha}A)_{\mu}$ for each α. To obtain a homogeneous and isotropic stress-energy tensor, following [31] we choose

$$ ({}^{\alpha}A)_{a} = A_{\gamma}(t)\delta^{\alpha}_{a}, \qquad ({}^{\alpha}A)_{t} = 0, \tag{2.7} $$

i.e., we take the three vector potentials to be mutually orthogonal, and impose that they share the same time dependent length. This choice gives a field strength where the only nonzero components are

$$ ({}^{\alpha}F)_{ta} = -({}^{\alpha}F)_{at} = \partial_{t}A_{\gamma}\delta^{\alpha}_{a}. \tag{2.8} $$

Given the metric (2.3), the Lagrangian density of the fields is

$$ {}^{\alpha}\mathcal{L} = \frac{a}{2N}(\partial_{t}A_{\gamma})^{2}, \tag{2.9} $$

and then the canonical momentum of the vector field is given by

$$ {}^{\alpha}\mathrm{P} = \frac{\delta({}^{\alpha}\mathcal{L})}{\delta(\partial_{t}{}^{\alpha}A)} = \frac{a}{N}({}^{\alpha}\Pi)^{\mu}, \tag{2.10} $$

where we have introduced

$$ ({}^{\alpha}\Pi)^{\mu} = (\partial_{t}A_{\gamma})\delta^{\alpha\mu} \equiv \Pi_{\gamma}\delta^{\alpha\mu}. \tag{2.11} $$

A subsequent Legendre transform gives the Hamiltonian density for one of the $U(1)$ species,

$$ {}^{\alpha}\mathcal{H} = \frac{1}{2a}\Pi_{\gamma}^{2}, \tag{2.12} $$

and the Poisson bracket between A_{γ} and Π_{γ} is determined by the induced symplectic structure

$$ \begin{aligned}\Omega(\delta_1,\delta_2) &= \sum_{\alpha=1}^{3}\int_{\Sigma}(\delta_1({}^{\alpha}A)_{\mu}\delta_2({}^{\alpha}\Pi)^{\mu} - \delta_2({}^{\alpha}A)_{\mu}\delta_1({}^{\alpha}\Pi)^{\mu}) \\ &= 3(\delta_1 A_{\gamma}\delta_2\Pi_{\gamma} - \delta_2 A_{\gamma}\delta_1\Pi_{\gamma}).\end{aligned} \tag{2.13} $$

The (appropriately regularized) integral over the spatial Cauchy slice Σ can be performed trivially due to homogeneity, and the overall factor of the volume of the space can be absorbed into the definition of the fields.[4] The Poisson bracket following from the induced symplectic structure is

$$ \{A_{\gamma}, \Pi_{\gamma}\} = \frac{1}{3}. \tag{2.14} $$

Finally, the total Hamiltonian density matter term is simply given by the sum of the three individual Hamiltonian densities,

$$ \mathcal{H}_{m} = \sum_{\alpha=1}^{3}{}^{\alpha}\mathcal{H} = \frac{3}{2a}\Pi_{\gamma}^{2}, \tag{2.15} $$

from which it is possible to calculate the energy density ρ and the pressure P of the universe matter content:

$$ \rho = \frac{\mathcal{H}_{m}}{\sqrt{q}} = \frac{3\Pi_{\gamma}^{2}}{2a^{4}}, \tag{2.16} $$

$$ P = -\frac{\partial\mathcal{H}_{m}}{\partial\mathrm{Vol}} = -\frac{\partial\mathcal{H}_{m}}{\partial a^{3}} = \frac{\Pi_{\gamma}^{2}}{2a^{4}}. \tag{2.17} $$

This implies in particular the relation $P = \rho/3$, just as one would expect for a radiation-dominated universe.

Alternatively, one can determine P and ρ by evaluating the stress energy tensor [31]. That method also has the advantage of explicitly showing that the stress energy tensor is that of a homogeneous and isotropic perfect fluid.

B. The gravitational sector

Since we embed the matter fields discussed above in the isotropic flat spacetime, the geometrical degrees of freedom are the scale factor a and its canonical momentum $\Pi_{(a)}$ with the Poisson bracket $\{a, \Pi_{(a)}\} = 1$. These variables (together with the matter degrees of freedom) suffice for describing this symmetry-reduced system (for details, see for example [36]). However, there is another pair of conjugate variables that is more convenient for LQC (see Sec. III and [3,4]) and which provide an equivalent description at the classical level, these variables are (proportional to) the oriented volume ν and its momentum b,

$$ \nu = \frac{a^{3}}{\alpha}, \qquad \alpha = 2\pi\gamma\ell_{\mathrm{Pl}}^{2}\sqrt{\Delta}, \tag{2.18a} $$

[4]The integral has to be regularized as the space is noncompact. This is done by introducing an infrared regulator, a compact comoving spatial region [33] (here a cubic cell $\mathcal{V}$ known as the *fiducial cell*) and subsequently ensuring that the resulting description admits a consistent regulator removal limit [3,11,34]. See also the discussion in [35].

$$b = -\frac{2\alpha^{\frac{1}{3}}}{3\hbar}\cdot\frac{\Pi_{(a)}}{|\nu|^{2/3}} = \frac{\alpha}{2\pi\ell_{\rm Pl}^2}H,$$
$$\{\nu, b\} = -\frac{2}{\hbar}, \tag{2.18b}$$

where the proportionality factor α contains the Barbero-Immirzi parameter γ [37] and the smallest nonzero eigenvalue of the LQG area operator Δ. Δ is often called the area gap and is of the order $\Delta \sim \ell_{\rm Pl}^2$ [38] (note that it has dimensions of area). The momentum b is proportional to the Hubble parameter H in the classical theory.

In the variables (v, b) the gravitational term of the Hamiltonian constraint density takes the form

$$\mathcal{H}_g = -\frac{\pi G}{3}\frac{\Pi_{(a)}^2}{a} = -\frac{3\pi G\hbar^2}{2\alpha}|\nu|b^2. \tag{2.19}$$

Together with the matter Hamiltonian density (2.15), $\mathcal{H}_g$ defines the classical dynamics of the system.

C. Classical dynamics

The classical dynamics of this model is generated by the Hamiltonian constraint term in the canonical action

$$N\mathcal{C}_H = \int_{\mathcal{V}} N[\mathcal{H}_g + \mathcal{H}_m], \tag{2.20}$$

where the gravitational and matter terms are given by (2.19) and (2.15), respectively. The physical trajectories lie on the surface

$$N\mathcal{C}_H = 0. \tag{2.21}$$

Note that the integration in (2.20) should in principle be performed over the entire constant time slice Σ, however such an integral would diverge due to homogeneity and noncompactness of the slice. A standard way of removing this divergence is the introduction of an infrared regulator: a compact region $\mathcal{V}$ of constant volume in comoving coordinates. Here for the sake of simplicity we choose $\mathcal{V}$ to be the cubical cell of edges generated by the vectors $\partial_x, \partial_y, \partial_z$ and of unit volume with respect to the line element $\mathrm{d}x^2 + \mathrm{d}y^2 + \mathrm{d}z^2$. The equations of motion (presented below) do not depend on the choice of the fiducial cell, and so it follows that the physical results do not depend on the size of the cell and the limit of removing the regulator is trivial in the classical theory. Note however that this is not the case in the quantum theory where taking the limit of $\mathcal{V} \to \mathbb{R}^3$ is not trivial, see [35,39] for more detailed discussions on this point. Nonetheless, this limit exists and the resulting quantum theory is independent of the initial choice of the fiducial cell.

Performing the (regulated) integral in (2.20) we arrive at the following form of the constraint,

$$\mathcal{C}_H = -\frac{3\pi G\hbar^2}{2\alpha}|\nu|b^2 + \frac{3}{2|\alpha\nu|^{1/3}}\Pi_\gamma^2. \tag{2.22}$$

So far the choice of the lapse N remains open, however in the quantum theory we will want to deparametrize the system with respect to the matter field in order to use A_γ as a clock. To synchronize the classical time with that clock, we choose $N = a(t) = \alpha|\nu|^{1/3}$ and denote the resulting time variable η. This choice corresponds to working in conformal time, and the resulting constraint reads

$$N\mathcal{C}_H = -\frac{3\pi G\hbar^2}{2\alpha^{2/3}}|\nu|^{4/3}b^2 + \frac{3}{2}\Pi_\gamma^2. \tag{2.23}$$

The equations of motion are the Hamilton-Jacobi equations which in this case consist of the following set of four coupled ordinary differential equations,

$$\frac{\mathrm{d}v}{\mathrm{d}\eta} = \frac{6\pi G\hbar}{\alpha^{2/3}}|\nu|^{4/3}b,$$
$$\frac{\mathrm{d}b}{\mathrm{d}\eta} = -\frac{4\pi G\hbar}{\alpha^{2/3}}\mathrm{sgn}(\nu)|\nu|^{1/3}b^2, \tag{2.24a}$$

$$\frac{\mathrm{d}A_\gamma}{\mathrm{d}\eta} = \Pi_\gamma, \qquad \frac{\mathrm{d}\Pi_\gamma}{\mathrm{d}\eta} = 0. \tag{2.24b}$$

These equations are equivalent to the usual Friedmann equations and are easily solved.

The matter degrees of freedom are determined by (2.24b): the momentum of the electromagnetic field is a constant of the motion and A_γ grows linearly in conformal time

$$\Pi_\gamma = \text{const},$$
$$A_\gamma(\eta) = \Pi_\gamma\eta + \Pi_o, \tag{2.25}$$

where Π_o is a free constant of integration.

The dynamics of (v, b) are determined by (2.24a) and can be found in two steps: first we note that the equation for an auxiliary variable $f := b|v|^{1/3}$ decouples from the system and so can easily be solved. Then, the (v, b) variables can be found once the solution f is plugged back into (2.24a) with the result

$$\nu(\eta) = \frac{(4\pi G)^{3/2}}{\alpha}\Pi_\gamma^3(\eta - \eta_o)^3, \tag{2.26a}$$

$$b(\eta) = \frac{\alpha}{2\pi G\hbar\sqrt{4\pi G}}\cdot\frac{1}{\Pi_\gamma(\eta - \eta_o)^2}, \tag{2.26b}$$

where η_o is a constant of integration corresponding to the moment of initial/final singularity.[5] Note that there is another constant of integration that is fixed by enforcing the constraint $N\mathcal{C}_H = 0$.

The monotonicity of $A_\gamma(\eta)$ allows us to eliminate the time dependence from the equations of motion by reparametrizing the evolution in terms of A_γ and thus use the vector potential as an internal clock,

$$\nu(A_\gamma) = \frac{(4\pi G)^{3/2}}{\alpha}(A_\gamma - A_o)^3, \tag{2.27a}$$

$$b(A_\gamma) = \frac{\alpha}{2\pi G\hbar\sqrt{4\pi G}} \cdot \frac{\Pi_\gamma}{(A_\gamma - A_o)^2}, \tag{2.27b}$$

where $A_o = \Pi_o + \Pi_\gamma \eta_o$. A_o then represents the "initial time" where the big-bang or big-crunch singularity occurs, according to the A_γ clock.

Finally, the energy density and pressure can be determined from Eqs. (2.16) and (2.17):

$$\rho = \frac{3}{32\pi^2 G^2 \Pi_\gamma^2 (\eta - \eta_o)^4} = \frac{3\Pi_\gamma^2}{32\pi^2 G^2 (A_\gamma - A_o)^4}, \tag{2.28}$$

$$P = \frac{1}{32\pi^2 G^2 \Pi_\gamma^2 (\eta - \eta_o)^4} = \frac{\Pi_\gamma^2}{32\pi^2 G^2 (A_\gamma - A_o)^4} = \frac{\rho}{3}. \tag{2.29}$$

III. THE QUANTUM THEORY

The procedure of quantizing (within the LQC framework) the classical system specified in the previous section is a direct analog of the procedure used for isotropic systems with a scalar field [3,11]. Therefore we recall it here only briefly, focusing mainly on the differences with respect to previous treatments and on the specific steps where quantization ambiguities force us to make particular choices.

A. The Dirac program

In general the process is an application of the Dirac program: first the constrained system is quantized while ignoring the constraints (the so-called *kinematical* quantization), then the constraints are defined as quantum operators, and finally the space of physical states is constructed out of the kernel of the quantum constraint operators. In this setting, meaningful physical quantities are represented by *partial observables* [30]. Let us start by recalling the kinematical quantization.

1. The kinematical Hilbert space

In this step, following the majority of works in LQC, we implement a hybrid approach, quantizing the geometry degrees of freedom via a polymeric quantization while using the standard quantum mechanical tools for the matter sector [40]. Thus, the kinematical Hilbert space is a product $\mathcal{H}_{\rm kin} = \mathcal{H}_{\rm gr} \otimes \mathcal{H}_A$ of the gravitational and matter Hilbert spaces.

The gravitational Hilbert space is the space of square-summable functions on the Bohr compactification of the real line (the space of almost periodic functions) $\mathcal{H}_{\rm gr} = L^2(\bar{\mathbb{R}}, \mathrm{d}\mu_{\rm Bohr})$. A convenient basis for this Hilbert space is formed by the eigenfunctions of the $\hat{v}$ operator,[6] the quantum counterpart of the variable v introduced in (2.18). The inner product on $\mathcal{H}_{\rm gr}$ is discrete,

$$\langle v|v'\rangle = \delta_{v,v'}, \tag{3.1}$$

where however v runs through the whole real line. As a consequence, $\mathcal{H}_{\rm gr}$ is nonseparable.

Normalizable states on $\mathcal{H}_{\rm gr}$ are represented by the wave function $\psi(v)$,

$$|\psi\rangle = \sum_{v\in\mathbb{R}} \psi(v)|v\rangle, \qquad \sum_{v\in\mathbb{R}} |\psi(v)| < \infty. \tag{3.2}$$

We will require that operators acting within this space be well defined on the domain $\mathcal{D}_{\rm gr}$ of *finite* linear combinations of $|v\rangle$.

As the basic operators defined on a dense domain in $\mathcal{H}_{\rm gr}$ we choose the operator $\hat{v}$ (proportional to the volume of the chosen comoving region of space) and the $U(1)$ unit shift operator $\hat{N}$ such that

$$\hat{v}|v\rangle = v|v\rangle, \qquad \hat{N}|v\rangle = |v+1\rangle. \tag{3.3}$$

The standard elementary operators of isotropic LQC—namely, the triad flux $\hat{p}$ across a face of the fiducial cell and the $SU(2)$ holonomy h_λ along a straight line of fiducial length λ—can be expressed in terms of $\hat{v}, \hat{N}$ [3,4].

The matter Hilbert space is the standard Lebesgue space $\mathcal{H}_A = L^2(\mathbb{R}, \mathrm{d}A_\gamma)$. As a basis we choose the generalized eigenstates $(A_\gamma|$ of the field operator $\hat{A}_\gamma$. States are represented by square-integrable wave functions $\psi(A_\gamma) := (A_\gamma|\psi\rangle$ and the basic operators are

$$\hat{A}_\gamma \psi(A_\gamma) = A_\gamma \psi(A_\gamma), \tag{3.4a}$$

[5]The solutions ((2.25), (2.26)) contain two branches: $(\eta > \eta_o)$ representing the expanding universe starting at the initial singularity $\eta = \eta_o$ and $(\eta < \eta_o)$ representing the universe contracting to the final singularity at $\eta = \eta_o$. Due to the irregularity of the equations of motion at $\eta = \eta_o$ there is no unique extension of the solution across the point $\eta = \eta_o$, although there is a unique analytic extension through that point.

[6]Note that from the $\hat{v}$ operator, it is possible to construct the operator $\hat{p} = \mathrm{sgn}(v)|\alpha\hat{v}|^{2/3}$, which corresponds to the flux of the densitized triad across one of the faces of the fiducial cell.

$$\hat{\Pi}_\gamma \psi(A_\gamma) = -\frac{i\hbar}{3}\frac{\mathrm{d}}{\mathrm{d}A_\gamma}\psi(A_\gamma); \tag{3.4b}$$

the domain on which we require the operators to be well defined is the Schwartz space $\mathcal{S}(\mathbb{R})$.

2. The Hamiltonian constraint operator

The next step in the Dirac program is the construction of the quantum operator representing the Hamiltonian constraint (2.23) and composed of the basic kinematical operators defined in (3.3) and (3.4). The procedure, while a bit complicated, is well described in the literature, see for example [3,11]. To capture the properties of full LQG we start by expressing the constraint (2.23) in terms of the $SU(2)$ holonomies A_a^i and densitized triads E_i^a directly. Next the constraint is regularized following the prescription given by Thiemann [41]. In particular, the field strength (i.e., the curvature of the connection) is expressed in terms of a holonomy along a closed square loop of physical area equal to the lowest nonzero eigenvalue of the area operator in LQG (relevant for LQC) $\Delta = 4\sqrt{3}\pi\gamma\ell_{\mathrm{Pl}}^2$. As a result the gravitational part of the constraint is expressed in terms of the holonomy functions and the volume, which next are promoted to composite operators expressed in terms of the operators (3.3). The matter part of the constraint does not need any special treatment and can be immediately expressed in terms of the operators (3.4).

The last step listed here involves some ambiguity due to different factor-ordering choices that are possible. Here we choose a particularly convenient factor-ordering motivated by studies of the anisotropic Bianchi I cosmology [11] which involves a specific treatment of the sign function and simplifies the resulting physical Hilbert space structure [42]. The final form of the operator is[7]

$$\widehat{NC}_H = \Theta \otimes \mathbb{1} + \mathbb{1} \otimes \frac{\partial^2}{\partial A_\gamma^2}, \tag{3.5}$$

where the operator Θ (also called the evolution operator) takes the form

$$\begin{aligned}\Theta\Psi(\nu; A_\gamma) = -\frac{9(2\pi\gamma\sqrt{\Delta})^{1/3}}{32\gamma\sqrt{\Delta}\hbar}&|\nu|^{1/3}[s_-(\nu-2)s_-(\nu)|\nu-4|^{1/3}|\nu-2|^{2/3}\Psi(\nu-4;A_\gamma)\\ &-(s_-^2(\nu)|\nu-2|^{2/3}+s_+^2(\nu)|\nu+2|^{2/3})|\nu|^{1/3}\Psi(\nu;A_\gamma)\\ &+s_+(\nu+2)s_+(\nu)|\nu+4|^{1/3}|\nu+2|^{2/3}\Psi(\nu+4;A_\gamma)],\end{aligned} \tag{3.6}$$

where $s_\pm(\nu) = \mathrm{sgn}(\nu \pm 2) + \mathrm{sgn}(\nu)$. This particular form of Θ has several convenient properties:

(1) The zero volume state $|\nu = 0\rangle$ decouples under the action of $\hat{\mathcal{C}}_H$.
(2) Due to presence of the $s_\pm(\nu)$ terms the sectors $\nu > 0$ and $\nu < 0$ decouple.
(3) Since Θ is a difference operator coupling only points in ν separated by 4, one can split the support of $\mathcal{H}_{\mathrm{gr}}$ elements onto independent sets $\nu = \epsilon + 4n$ (preserved under the action of $\hat{\mathcal{C}}_H$), where $n \in \mathbb{Z}$ and $\epsilon \in (0, 4]$.

The first property implies that we can exclude the singular $|v = 0\rangle$ states from the support of the wave function, showing that the singularity is resolved at the quasi-kinematical level.

At this point it is useful to note one more important property of the model, namely that it does not feature parity violating interactions. In consequence the triad reflection (here represented by $\nu \mapsto -\nu$) is a large symmetry and the subspaces of symmetric and antisymmetric (with respect to that reflection) states are superselection sectors. As a consequence one can choose just one of them and then, due to properties 1 and 2 above, restrict the support of the wave function to $\nu > 0$.

That restriction, together with property 3, allows us to divide $\mathcal{H}_{\mathrm{gr}}$ into superselection sectors consisting of the projections of $\psi \in \mathcal{H}_{\mathrm{gr}}$ onto the positive semilattices

$$\mathcal{L}_\epsilon = \{v \in \mathbb{R}\colon\ v = \epsilon + 4n, n \in \mathbb{N}\}, \tag{3.7}$$

and work with just a single superselection sector, provided that these sectors are also preserved by the chosen set of observables (which as we shall see below is the case). Of course, it is important to verify that the physics does not depend on the choice of the superselection sector, as there does not exist any principle that could justify one choice over another.

One justification for working with a single sector is that while the entire Hilbert space $\mathcal{H}_{\mathrm{gr}}$ is not separable, each superselection sector $\mathcal{H}_{\mathrm{gr},\epsilon} := \{\psi|_{\mathcal{L}_\epsilon}; \psi \in \mathcal{H}_{\mathrm{gr}}\}$ is. An alternative possibility to construct a separable Hilbert space is to use the construction given in Appendix C of [44] or to exploit the natural fibration of $\mathcal{H}_{\mathrm{gr}}$ and the Lebesgue measure on the fiber space inherited from superselection labels. The latter method leads to the fiber-integral Hilbert space which is again separable [26,45]. For the remaining part of this paper we choose the first approach and work with one superselection sector.

[7]It is defined analogously to the prescription provided for the system with a massless scalar field in [43] and denoted there as *sMMO*. See [43] for its description and a comparison with other factor-ordering choices.

Upon restriction to a positive semilattice $\mathcal{L}_\epsilon$, the evolution operator Θ [whose action is given in (3.6)] can be simplified to

$$\begin{aligned}\Theta\Psi(\nu;A_\gamma) &= f^+(\nu)\Psi(\nu+4;A_\gamma) + f^o(\nu)\Psi(\nu;A_\gamma)f^-(\nu)\Psi(\nu-4;A_\gamma)\\ &= -\frac{9(2\pi\gamma\sqrt{\Delta})^{1/3}}{8\gamma\sqrt{\Delta}\hbar}\nu^{1/3}\times[\theta(\nu-4)(\nu-4)^{1/3}(\nu-2)^{2/3}\Psi(\nu-4;A_\gamma)\\ &\quad-(\theta(\nu-2)(\nu-2)^{2/3}+(\nu+2)^{2/3})\nu^{1/3}\Psi(\nu;A_\gamma)\\ &\quad+(\nu+4)^{1/3}(\nu+2)^{2/3}\Psi(\nu+4;A_\gamma)],\end{aligned} \tag{3.8}$$

where $\theta(\nu)$ is the Heaviside step function.

From this one can infer several important properties:

(a) Since $f^\pm, f^o$ are real functions, the operator is real.

(b) All (generalized) eigenfunctions are solutions to the second order difference equation

$$\Theta\psi_\lambda(\nu) = \lambda\psi_\lambda(\nu). \tag{3.9}$$

(c) Due to the presence of θ functions in (3.8), $\psi_\lambda(\epsilon+4)$ is uniquely determined by $\psi_\lambda(\epsilon)$, therefore all the eigenspaces are 1-dimensional and the spectrum $\mathrm{Sp}(\Theta)$ is nondegenerate.

(d) Due to the reality of the operator, all of its eigenfunctions are real up to a global phase.

(e) By construction, the operator is symmetric and positive definite on its domain $\mathcal{D}$.

(f) By direct inspection of its deficiency functions (using numerical methods described in [3,43] and the asymptotic analysis of [46], further applied in Sec. B 2), one can show that Θ is essentially self-adjoint.

(g) By exploring the asymptotic properties of the generalized eigenfunctions corresponding to the positive eigenvalues $\lambda = \omega^2$ and the spectral properties of the WDW analog of Θ, one can show that[8] the spectrum of Θ is purely continuous and $\mathrm{Sp}(\Theta) = \mathbb{R}^+$.

These properties will be essential in constructing the physical Hilbert space and probing the dynamics of the system.

3. The physical Hilbert space

In the Dirac program, the space of physical states is defined as the set of states annihilated by the quantum constraint operator, that is $\widehat{NC}_H\Psi = 0$. Thus, these states must satisfy the equation

$$-\frac{\partial^2}{\partial A_\gamma^2}\Psi(\nu;A_\gamma) = \Theta\Psi(\nu;A_\gamma), \tag{3.10}$$

where the action of Θ is given in (3.8).

A systematic way to find this space is the so-called group averaging method [48], where one builds an antilinear rigging map that provides an "extractor operator" $\mathcal{P}$ which projects the kinematical state Φ onto the physical wave function Ψ:

$$\Psi(\nu,A_\gamma) = [\mathcal{P}\Phi](\nu,A_\gamma) = \int \mathrm{d}t e^{it\widehat{NC}_H}\Phi(\nu,A_\gamma). \tag{3.11}$$

Using the spectral properties of Θ and $\partial^2_{A_\gamma}$ and following the algorithm specified in [44], one can easily determine the form of the physical states,

$$\begin{aligned}\Psi(\nu,A_\gamma) &= \int_{\mathbb{R}^+}\mathrm{d}k\tilde{\Psi}^+(k)e_k(\nu)e^{i\omega(k)A_\gamma}\\ &\quad+\int_{\mathbb{R}^+}\mathrm{d}k\tilde{\Psi}^-(k)\bar{e}_k(\nu)e^{-i\omega(k)A_\gamma},\end{aligned} \tag{3.12}$$

where $\tilde{\Psi}^\pm(k)\in L^2(\mathbb{R}^+,\mathrm{d}k)$ are the spectral profiles of what we shall call the positive and negative "frequency" components,[9] the norm is $\|\Psi\|^2 = \|\tilde{\Psi}^+\|^2_{L^2} + \|\tilde{\Psi}^-\|^2_{L^2}$ and e_k are the Dirac delta normalized (generalized) eigenfunctions of Θ that can be chosen to be real and with $e_k(\epsilon) > 0$,

$$\Theta e_k = \omega^2(k)e_k, \tag{3.13}$$

with the relation between the "wave" label k and the "frequency" ω being given by[10]

$$\omega_k^2 = 2\frac{(2\pi\gamma\sqrt{\Delta})^{1/3}}{\gamma\sqrt{\Delta}\hbar}k^2. \tag{3.14}$$

Using the similarity of (3.10) to the Klein-Gordon equation (with A_γ being the analog of time) one can conclude that the first and second components of (3.12) are the "frequency" superselection sectors, of which we select the first one. In this case Eq. (3.10) can be rewritten in the form

[8]Unfortunately, as the leading power of v in f for large ν is not an integer, the mathematically precise proof of this property presented in [47] for a massless scalar field cannot be adapted to the case of a Maxwell field that is considered here.

[9]The reason for choosing this nomenclature will become clear in the next section.

[10]At the moment this relation is arbitrary as we can relabel k, although this particular choice is justified by the asymptotic properties of e_k analyzed in Appendix B 2.

$$-i\frac{\partial}{\partial A_\gamma}\Psi(\nu;A_\gamma)=\sqrt{\Theta}\Psi(\nu;A_\gamma). \tag{3.15}$$

Finally, the physical states are

$$\Psi(\nu,A_\gamma)=\int_{\mathbb{R}^+}\mathrm{d}k\Psi(k)e_k(\nu)e^{i\omega(k)A_\gamma}, \tag{3.16}$$

and the physical inner product is

$$\langle\Psi|\Psi'\rangle=\int_{\mathbb{R}^+}\mathrm{d}k\overline{\Psi}(k)\Psi'(k). \tag{3.17}$$

The problem with this construction is the standard one that arises in constrained systems: this gives a frozen time evolution where physical states represent entire "histories" of the universe. Providing a physically meaningful and nontrivial notion of evolution is not straightforward.

B. Physical evolution

There are two well-developed methods that can be used in order to define meaningful dynamics in a constrained system, namely *deparametrization* and the *partial observable* formalism. For the system considered here these two methods are equivalent, although this equivalence does not hold in general. In fact, even in isotropic LQC there exist systems where these two approaches give distinct results [49].

1. Deparametrization

The principal idea behind deparametrization is the observation that all the information about the physical state $|\Psi\rangle$ is contained within a single constant A_γ slice of the wave function. Indeed, the Schrödinger-like equation (3.15) implies that given an initial slice $\Psi(\cdot,A_\gamma)\in\mathcal{H}_{\mathrm{gr}}$, we can reproduce the entire physical state via the unitary transformations

$$\begin{aligned}\Psi(\nu,A_\gamma)&=U_{A_{\gamma_o},A_\gamma}\Psi(\nu,A_{\gamma_o})\\&=e^{i\sqrt{\Theta}(A_\gamma-A_{\gamma_o})}\Psi(\nu,A_{\gamma_o}).\end{aligned} \tag{3.18}$$

The structure of the physical states (3.16) and the properties of Θ (namely its self-adjointness and positive definiteness) also imply the equivalence between the physical inner product and the gravitational kinematical inner product on constant A_γ slices

$$\forall\ A_\gamma\in\mathbb{R}\colon\ \langle\Psi|\Psi'\rangle_{\mathrm{phy}}=\langle\Psi(\cdot,A_\gamma)|\Psi'(\cdot,A_\gamma)\rangle_{\mathrm{gr}}, \tag{3.19}$$

which allows us to interpret A_γ as an *emergent time* and use it as an evolution parameter. We can thus define the dynamics as the unitary mapping

$$\mathbb{R}\ni A_\gamma\mapsto\Psi(\cdot,A_\gamma)\in\mathcal{H}_{\mathrm{gr}}. \tag{3.20}$$

A convenient consequence of this approach is the fact that any self-adjoint operator on $\mathcal{H}_{\mathrm{gr}}$ evaluated at a particular "time" A_γ automatically becomes a physical observable.

This property allows us to easily show that there exists an upper bound on the physical matter energy density. To show this, we start by defining in the kinematical Hilbert space the operator corresponding to the matter energy density defined in (2.16),

$$\hat{\rho}=\frac{3}{2}[(\widehat{|\alpha\nu|})^{-1/3}\hat{\Pi}_\gamma(\widehat{|\alpha\nu|})^{-1/3}]^2. \tag{3.21}$$

As the zero-volume states have decoupled, the inverse $|\alpha\nu|$ operator is well defined. This form of the $\hat{\rho}$ operator clearly shows that it is a positive-definite operator as it is the square of a self-adjoint operator. Therefore, all of its eigenvalues will be real and greater than or equal to zero.

In addition, for states annihilated by the constraint (3.10), the action of this operator is exactly balanced via (3.15) by the gravitational energy operator which (after selecting a convenient factor ordering) can be written as [4,8,50]

$$\rho_G=-\tilde{\rho}\otimes\mathbb{1},\qquad\tilde{\rho}=\rho_c\sin^2(b), \tag{3.22}$$

where the critical energy density equals

$$\rho_c=\frac{3}{8\pi\gamma^2\Delta G}, \tag{3.23}$$

and is of the order of the Planck energy density.[11]

Since the operator $\tilde{\rho}$ is self-adjoint on $\mathcal{H}_{\mathrm{gr}}$, in the deparametrization picture it becomes a physical observable. On the other hand, its form implies immediately that

$$\mathrm{Sp}(\tilde{\rho})=[0,\rho_c]. \tag{3.24}$$

Therefore, the physical matter energy density is bounded from above by ρ_c.

Note that in order to determine whether this upper bound is saturated one needs to study in detail the dynamical evolution of the state in the sense of (3.20).

2. The partial observable formalism

An alternative way to define the dynamics is provided by the formalism of partial observables originally introduced in [30] (see also [52] for a critical analysis of the formalism). The goal is to construct Dirac observables acting within the physical Hilbert space, where these observables correspond to measuring one property of the state with respect to another. Here the natural choice is to

[11] In the numerical studies we took the value determined via (3.23) for the value $\gamma=0.2375\ldots$ determined in [51], which gives $\rho_c\approx 0.41\rho_{\mathrm{Pl}}$.

measure quantities with respect to the vector potential A_γ, which will act as a relational clock.

These observables can be constructed systematically out of observables in the kinematical Hilbert space via group averaging [49]. In particular, in our case, given a self-adjoint operator $\hat{O}$ on $\mathcal{H}_{\rm gr}$, the group averaging of the "seed" operator $\hat{O} \otimes \delta(\hat{A}_\gamma - T)$ gives the Dirac observable $\hat{O}_T$

$$\hat{O}_T \Psi(\nu, A_\gamma) = e^{i\sqrt{\Theta}(A_\gamma - T)} \hat{O} \Psi(\nu, T), \tag{3.25}$$

which is just a completion of the (result of the) action of the gravitational kinematical observable $\hat{O}$ to the physical state (3.16) via the unitary transformation (3.18). In consequence, in this setting the formalism is equivalent to the deparametrization picture.

Using this procedure we construct the following set of observables: the volume $\hat{V}$ at the "time" $A_\gamma|_0$ and the momentum $\hat{\Pi}_\gamma$ (which is a constant of the motion), given by

$$\widehat{V(A_\gamma|_0)}\Psi(\nu; A_\gamma) = e^{i\sqrt{|\Theta|}(A_\gamma - A_\gamma|_o)}(2\pi\gamma\sqrt{\Delta}\ell_{\rm Pl}^3) \times \nu\Psi(\nu; A_\gamma|_0), \tag{3.26a}$$

$$\hat{\Pi}_\gamma \Psi(\nu; A_\gamma) = -i\hbar \frac{\partial}{\partial A_\gamma} \Psi(\nu; A_\gamma). \tag{3.26b}$$

3. Dynamics

Either one of the two formalisms discussed in the previous sub-subsections can be used to determine the dynamics of this system. To achieve this goal we need to perform two tasks: the evaluation of the wave functions and the computation of the expectation values and the dispersions of the relevant observables.

To determine the wave function $\Psi(\nu, A_\gamma)$ as given in (3.16) one needs to know the explicit form of e_k. Unfortunately the form of Θ is not simple enough to easily determine its analytic form. We therefore resort to numerical methods, applying directly the techniques specified in [43,44]: solving directly (3.13), which after substituting the form (3.8) of Θ becomes a second[12] order difference equation, and normalizing the solution via its WDW limit analysis (see the discussion in Appendix B). The normalization procedure features the only difference with respect to the treatment of [43,44]. Namely, due to slightly more complicated structure of the WDW analog of our model and a lower order of convergence of e_k to its WDW component limit, we used the modified auxiliary basis functions (B20) instead.

The wave function itself is then determined via a direct numerical integration (using the Romberg method) of (3.16) (see again [43,44] for a detailed description of the method).

In the actual computations we used the Gaussian spectral profiles

$$\tilde{\Psi}(k) = N e^{-(k-k_o)^2/2\sigma^2} e^{ikA_\gamma^\star} \tag{3.27}$$

peaked about k_o and with $A_\gamma^\star$ selected to reproduce the value of expectation value of observable $\widehat{V(A_\gamma)} = V^\star$ for the chosen $V^\star$ at the chosen "initial time" $A_\gamma = A_\gamma^o$. In practice we use the formula following from the classical trajectory (2.27) which reproduces the desired result sufficiently well so long as the parameters satisfy $V^\star \gg |k^\star|\ell_{\rm Pl}^3$.

For the chosen profile (3.27) the expectation values and dispersion of $\hat{\Pi}_\gamma$ can be determined analytically,

$$\langle \hat{\Pi}_\gamma \rangle = |k_o|, \qquad \langle \Delta\hat{\Pi}_\gamma \rangle = \sigma. \tag{3.28}$$

To evaluate the analogous quantities for the observables $\widehat{V(A_\gamma)}$ we use the deparametrization picture, evaluating $\langle \Psi(\cdot, A_\gamma)|\hat{V}|\Psi(\cdot, A_\gamma)\rangle_{\rm gr}$ and $\langle \Psi(\cdot, A_\gamma)|\Delta\hat{V}|\Psi(\cdot, A_\gamma)\rangle_{\rm gr}$ by direct numerical summation (see again [43,44]).

In the studies performed the parameters were chosen from within the ranges $\Pi_\gamma \in [30, 1700](G\sqrt{\hbar})^{-1}$, $\Delta\Pi_\gamma/\Pi_\gamma \in [0.02, 0.1]$, $V(A_\gamma^o) \in [3.1 \times 10^3, 2.5 \times 10^4]\ell_{\rm Pl}^3$.

The results of the analysis (see Figs. 1 and 2) are fully analogous to the results of studies of the systems with a massless scalar field [3] and pressureless dust [8]:

(1) For as long as the energy density [evaluated as the expectation value of $\tilde{\rho}$ in (3.22)] is small in comparison to $\rho_{\rm Pl}$, the quantum trajectory follows the classical one.
(2) When the energy density reaches Planck scales the quantum gravity effects modify the trajectory and lead to a bounce at the critical density $\rho = \rho_c$. The modification can be heuristically understood as the result of a repulsive gravitational force originating from the underlying fundamental discreteness of space-time.

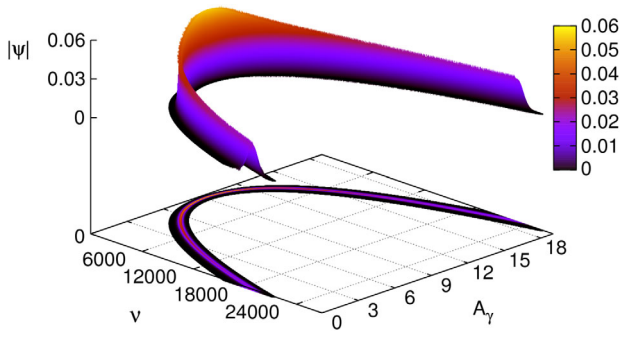

FIG. 1 (color online). An example of a physical state: forward evolution of the Gaussian (3.27) packet peaked about $\Pi_\gamma \approx 83.3(G\sqrt{\hbar})^{-1}$ and (at initial time $A_\gamma = 0$) about $\nu \approx 1.8 \times 10^4$.

[12]Its space of solutions is nonetheless 1-dimensional due to the orientation decoupling (see the discussion in Sec. III A 2).

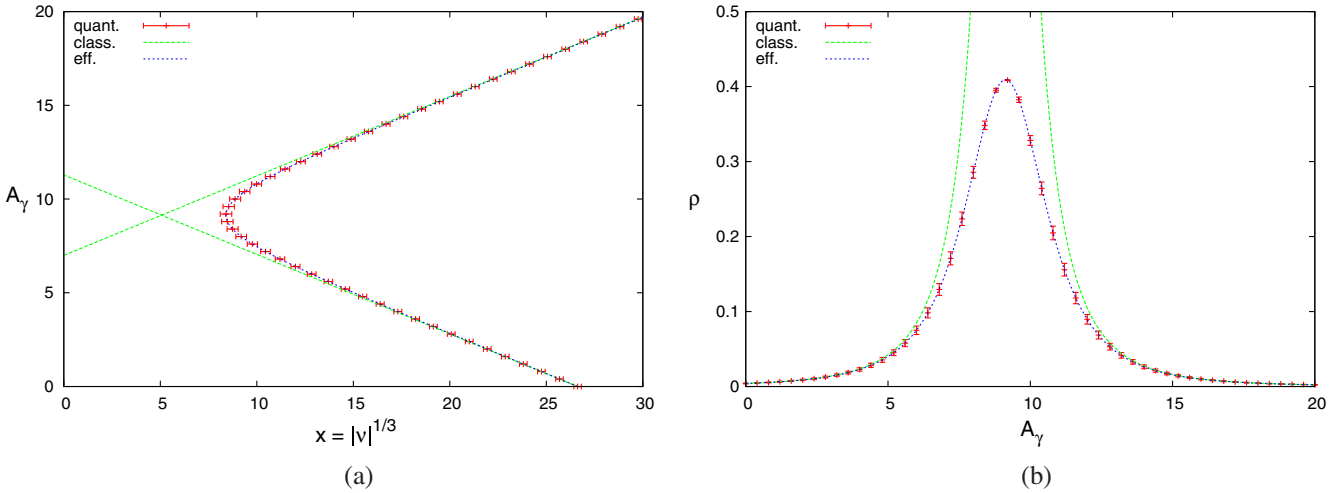

FIG. 2 (color online). The expectation values of the observables $\hat{x}|_{A_\gamma} = \widehat{|\nu|^{1/3}_{A_\gamma}}$ and $\hat{\rho}|_{A_\gamma}$ evaluated for the wave packet presented in Fig. 1 are compared with the classical trajectories and the evolution predicted by the effective dynamics discussed in Sec. V.

(3) The bounce is a transition epoch deterministically connecting two classical epochs of the universe's evolution, when the universe is contracting and expanding respectively.

In the case where the massless scalar field was the matter field, one of the nice features of the system was an asymptotic preservation of the semiclassicality. There, the spread of the state in the distant future is strongly bounded by its spread in the distant past (and vice versa) through precise triangle inequalities. It is therefore natural to test whether an analogous result can also be obtained in the model studied here. We address this issue in the next section.

IV. ASYMPTOTICS OF THE DYNAMICS

In studies of isotropic FLRW cosmologies with a massless scalar field (which can be used as a clock, just as A_γ) it has been shown that in the large ν limit all of the eigenfunctions of the LQC evolution operator—an analog of Θ (3.6)—converge to specific linear combinations of the eigenfunctions of the evolution operator arising in the Wheeler-DeWitt (WDW) quantization of the same system [3]. This property of the above-mentioned operator permits the modeling of the global LQC evolution as a certain form of "scattering" of WDW universes (wave packets) by polymeric quantum geometry effects [46]. In a very precise sense, the wave packets representing the LQC universe converged in the distant past and future to "incoming" (contracting) and "outgoing" (expanding) WDW wave packets respectively. A detailed study of this picture shows that there exist rigid relations (in the form of triangle inequalities) between the spreads of the LQC wave packet in its distant past and future [46].

This section is dedicated to developing and exploring this same scattering picture, but in the setting studied in this paper, namely a radiation-dominated universe. To achieve this, we first construct and study the WDW quantization of the radiation-dominated FRLW universe in Sec. IV A and its dynamics, focusing in particular on the issue of the uniqueness of the evolution and its relation with singularity resolution. Next, in Sec. IV B we employ the existence of a WDW limit of the LQC evolution operator to construct a scattering picture and then derive triangle inequalities relevant to the question of cosmic recall, analogous to those found in [46]. In order to provide a stream-lined presentation of this analysis—including the improvements necessary to handle Maxwell fields—Secs. IV A and IV B contain only a brief description of the calculation and results, while the details of the analysis can be found in Appendices A and B.

The triangle inequalities will allow us to provide a rigid bound on how much the spread of a wave function can grow from one side of the bounce to the other. Thus, this gives an answer to the question of cosmic recall in the following context: if the state is semiclassical on one side of the bounce, will it remain so on the other side? In the previous section, numerical studies showed that Gaussian states that are initially semiclassical remain sharply peaked throughout their entire evolution. However, determining how the spread of a generic state evolves requires stronger and more general methods, of which the scattering picture is a good example.

A. The Wheeler-DeWitt analog

The classical cosmological model given in Sec. II can be also quite easily quantized following the geometrodynamical methods of WDW quantum cosmology, by using the standard Schrödinger representation rather than the polymer one. The details of the WDW quantization procedure are presented in Appendix A. Here we briefly summarize the initial assumptions of the procedure and present the final result.

Since the WDW analog is to be ultimately used as an approximation to the asymptotics of LQC through a scattering picture, it is necessary to ensure that it is as close of an analog to our LQC model as is possible. Therefore, we directly repeat the procedure used in Sec. III, in particular by following the Dirac program. We further extend the configuration space to negative ν to ensure compatibility with LQC, and also choose same factor-ordering and symmetric superselection sector.

The first step of the Dirac program leads to the kinematical Hilbert space

$$\underline{\mathcal{H}}_{\rm kin} = \underline{\mathcal{H}}_{\rm gr} \otimes \mathcal{H}_A = L^2(\mathbb{R}^+, {\rm d}\nu) \otimes L^2(\mathbb{R}, {\rm d}A_\gamma). \quad (4.1)$$

The basic operators—quantum counterparts of variables ν, b—are now multiplication and differential operators respectively, and the quantum Hamiltonian constraint takes the form

$$\underline{\Theta} \otimes \mathbb{1} + \mathbb{1} \otimes \frac{\partial^2}{\partial A_\gamma^2}, \quad (4.2)$$

where the evolution operator $\underline{\Theta}$ is a second-order differential operator defined on the Schwartz space. The notation is chosen so that all objects in WDW theory are represented by same symbols as in LQC, although to differentiate them the WDW symbols are underlined.

Unfortunately, $\underline{\Theta}$ is not essentially self-adjoint. Rather, it admits a $U(1)$ family of self-adjoint extensions labeled by the parameter $\beta \in [0, \pi)$. The essential part of the spectrum of each extended operator $\underline{\Theta}_\beta$ is $\mathbb{R}^+ \cup \{0\}$ and is absolutely continuous. The physical sector of the theory (identified by group averaging) consists of states described by the wave functions

$$\underline{\Psi}(\nu, A_\gamma) = \int_{\mathbb{R}^+} {\rm d}k \tilde{\Psi}(k) e_{\beta,k}(\nu) e^{i\omega(k)A_\gamma}, \quad (4.3)$$

where the spectral profiles $\tilde{\Psi} \in L^2(\mathbb{R}^+, {\rm d}k)$, the frequency $\omega(k) \propto k$ is defined in (A10) and the normalized generalized basis functions $e_{\beta,k}$ have the form of the standing waves

$$e_{\beta,k}(\nu) = \frac{|\nu|^{-1/3}}{\sqrt{6\pi}} \cos[k|\nu|^{1/3} + \underline{\varphi}(\beta, k)] \quad (4.4)$$

and the extension-dependent phase shift is [see (A16)]

$$\underline{\varphi}(\beta, k) \coloneqq \arctan[\tan(\beta)/k]. \quad (4.5)$$

To study the dynamics of this WDW quantum theory, we can use either (i) the deparametrization procedure where the evolution is provided by the map $\mathbb{R} \ni A_\gamma \mapsto \Psi(\cdot, A_\gamma) \in \mathcal{H}_{\rm gr}$ [where the basis for each self-adjoint extension is given in (4.4) for $A_\gamma = 0$] and the self-adjoint operators $\underline{\hat{O}}$ on $\mathcal{H}_{\rm gr}$ are the physical observables, or (ii) the relational observables picture, where the Dirac observables (parametrized by T) are the families of operators acting on $\mathcal{H}_\beta$—where $\beta \in [0, \pi)$ denotes the one-parameter family of self-adjoint extensions—as

$$\underline{\hat{O}}_T : \Psi(\nu, A_\gamma) \mapsto e^{i\sqrt{\underline{\Theta}_\beta}(A_\gamma - T)} \underline{\hat{O}} \psi(\nu, A_\gamma = T). \quad (4.6)$$

In this case, for $\underline{\Theta}_\beta$, the two approaches are equivalent.

Here, for concreteness, we shall use the deparametrization procedure. As a convenient set of observables $\underline{\hat{O}}$ we choose

$$\underline{\hat{\Pi}}_\gamma = (-i\hbar/3)\partial_{A_\gamma}, \qquad \underline{\hat{x}} = \widehat{|\nu|^{1/3}}. \quad (4.7)$$

Note here that x is positive-definite. While $\underline{\hat{\Pi}}_\gamma$ is a constant of motion, the evolution of $\underline{\hat{x}}$ is nontrivial. It is easy to see that the evolution of the quantum universe is given by an incoming Klein-Gordon wave packet corresponding to the "pre-singularity" contracting universe, which upon approaching $x = 0$ is reflected (with a phase shift that depends on the self-adjoint extension and also k) back into an outgoing wave packet corresponding to the "post-singularity" expanding universe. Up to the dispersion of the wave packet, the quantum evolution follows the (extended) classical trajectory (2.26).

The exact form of the reflected wave packet depends on the chosen self-adjoint extension, and therefore knowledge of the extension label β (which is equivalent to specifying boundary conditions at $x = 0$) is necessary—in addition to knowing the initial state—to uniquely determine the evolution. In particular, $\beta = 0$ corresponds to a simple reflection (as would occur off an infinite potential barrier) and $\beta = \pi/2$ corresponds to a reflection with phase rotation π (i.e., sign change). However, all the values $\beta \in [0, \pi)$ are allowed and they correspond to the reflective conditions with a particular phase shift.[13]

The fact that the choice of the self-adjoint extension β affects the quantum dynamics shows that the singularity is not resolved in the WDW theory. This is because the choice of β is equivalent to setting boundary conditions at the singularity in order to evolve through the singularity "by hand"; for further discussion on this point, see [8].

B. Cosmic recall

The dynamics of this WDW model can be used to accurately describe the asymptotic dynamics in the distant future and past of the LQC model studied here, as well as provide the relation between these epochs via the application

[13]Note that the choice of β, which determines the reflection conditions of the eigenstates from the incoming to the outgoing mode, is completely unrelated to the choice of the symmetric superselection sector $\underline{\psi}(\nu) = \underline{\psi}(-\nu)$.

of the scattering picture originally introduced in [46]. The construction of the scattering picture for the model considered here, including the necessary extensions in order to handle a Maxwell field, is given in detail in Appendix B. The key points are the following:

(1) For any localized[14] LQC physical state $|\Psi\rangle$ there exist two unique WDW physical states $|\Psi_{\rm in}\rangle$ and $|\Psi_{\rm out}\rangle$ such that their dynamics in the distant past and future respectively converge (in the sense of expectation values and dispersions of $\hat{x}_{A_\gamma}$) with that of $|\Psi\rangle$, that is

$$\lim_{A_\gamma\to\pm\infty}[\langle\Psi|\hat{x}_{A_\gamma}|\Psi\rangle-\langle\underline{\Psi}_{\rm in/out}|\hat{x}_{A_\gamma}|\underline{\Psi}_{\rm in/out}\rangle_{\rm WDW}]=0, \tag{4.8a}$$

$$\lim_{A_\gamma\to\pm\infty}[\langle\Psi|\Delta\hat{x}_{A_\gamma}|\Psi\rangle-\langle\underline{\Psi}_{\rm in/out}|\Delta\hat{x}_{A_\gamma}|\underline{\Psi}_{\rm in/out}\rangle_{\rm WDW}]=0, \tag{4.8b}$$

and the expectation values and dispersions of $\hat{\Pi}_\gamma$ of all three states agree.

(2) The distant past and distant future dispersions of the WDW states are related via the triangle inequality

$$\lim_{A_\gamma\to\infty}\langle\Psi|\Delta\hat{x}_{A_\gamma}|\Psi\rangle\le\lim_{A_\gamma\to-\infty}\langle\Psi|\Delta\hat{x}_{A_\gamma}|\Psi\rangle+2\langle\Psi|\Delta(\partial_k\varphi(k))|\Psi\rangle, \tag{4.9}$$

where the function $\varphi(k)$ is the phase shift of the leading-order large ν limit of the basis functions $e_{\beta,k}$

$$e_{\beta,k}(\nu)=\frac{\sqrt{2}}{\sqrt{3\pi}|\nu|^{1/3}}\cos[k|\nu|^{1/3}+\varphi(k)]+O(\nu^{-4/3}). \tag{4.10}$$

In order to turn (4.9) into a useful relation (analogous to the one found in [46]) we must express $\partial_k\varphi(k)$ in terms of physically meaningful observables, or at least derive an upper bound. In order to derive an upper bound, it is necessary to resort to numerical analysis, as detailed in Appendix B 4.

The resulting bound—valid for all superselection sector labels ϵ and for states supported outside of the interval $[0,k_\star]$ with $k_\star\approx 0.15$—is

$$|\sqrt{k}\partial_k^2\varphi(k)|\le A/2, \tag{4.11}$$

where $A=-0.789\pm0.005$. Note that the domain in k where the bound holds is stronger for certain values of ϵ (see again Appendix B 4 for details), and in particular for $\epsilon=0$ the bound is valid for states supported on $k\in\mathbb{R}^+$.

As a direct consequence, within the domain of validity given above, it is possible to rewrite (4.9) as

$$\lim_{A_\gamma\to\infty}\langle\Psi|\Delta\hat{x}_{A_\gamma}|\Psi\rangle\le\lim_{A_\gamma\to-\infty}\langle\Psi|\Delta\hat{x}_{A_\gamma}|\Psi\rangle+A\langle\Psi|\Delta\sqrt{k}|\Psi\rangle, \tag{4.12}$$

where the only observable besides $\hat{x}_{A_\gamma}$ is $\sqrt{k}$, which is proportional to $\hat{\Pi}_\gamma{}^{1/2}$.

This triangle inequality gives a bound on how much the spread in $\hat{x}_{A_\gamma}$ can grow from the pre-bounce branch to the post-bounce branch. This shows the presence of cosmic recall: a moderately sharply-peaked state in the contracting branch cannot become wildly quantum in the expanding branch, and vice versa.

V. EFFECTIVE THEORY

An interesting and very useful result of LQC is that a classical theory, obtained by implementing the regularization of the Hamiltonian constraint but without quantizing it, describes the quantum dynamics of semiclassical states to a very good degree of precision (with an error well below the dispersion of the state) in many scenarios [3,5,7,39,53].[15] A systematic way to obtain this classical Hamiltonian constraint—called the *effective Hamiltonian constraint*—is by replacing the shift operators and powers of volume by their respective expectation values. The dynamics the effective Hamiltonian constraint generates are known as the *effective dynamics of LQC* and have been used extensively.

The effective equations are expected to provide an excellent approximation to the full quantum dynamics for those states that are sharply peaked. It has been shown that, for noncompact space-times (and also compact space-times whose spatial volume remains much larger than $\ell_{\rm Pl}^3$ at all times), a state which is initially sufficiently sharply peaked in the semiclassical limit will remain sharply peaked throughout its entire evolution, including at and around the bounce point where quantum gravity effects are strongest [39]. As the space-time of interest in this case is noncompact, the effective equations will indeed provide an

[14]Here by localized we mean a state for which the uncertainties of both the observables $\hat{\Pi}_\gamma$ and $\hat{x}_{A_\gamma}$ are finite in either the distant past or future.

[15]Although it is easy to construct the effective dynamics heuristically in many contexts of LQC—including the LQC of isotropic space-times with a Schrödinger quantization of the matter sector, as is being studied here—one cannot take this heuristic construction for granted in more complicated cosmologies. The details of the formulation of the quantum theory, neglected at the effective level, *do significantly affect* the genuine quantum dynamics and the existence of semiclassical sectors of the theory. For more details, see for example the discussion in [26]. Whether the domain of applicability of the effective dynamics in LQC includes more generic cosmologies than isotropic space-times with a Schrödinger quantization of the matter sector has not yet been determined.

excellent approximation to the full LQC dynamics of sharply peaked states throughout their entire evolution. This has been verified numerically for the radiation-dominated cosmology studied here, and the strong agreement between the effective equations and the full LQC dynamics can be seen in Fig. 2.

Following the procedure described above, the effective Hamiltonian constraint (in conformal time η) takes the form

$$\mathcal{C}_H^{\rm eff}(\eta) = -\frac{3\pi G\hbar^2}{2\alpha^{2/3}}|\nu|^{4/3}\sin^2 b + \frac{3}{2}\Pi_\gamma^2 = 0, \tag{5.1}$$

where it is possible to restrict our attention to the sector $\nu > 0$ without any loss of generality. One of the immediate consequences following from this equation is that the (classical) matter energy density, originally given by Eq. (2.16) takes the form

$$\rho = \frac{3}{8\pi G\gamma^2\Delta}\sin^2 b \leq \frac{3}{8\pi G\gamma^2\Delta} = \rho_c, \tag{5.2}$$

and thus ρ is bounded above by the critical energy density, just as in the quantum theory.

The equations of motion generated by $\mathcal{C}_H^{\rm eff}$ are (in the sector $\nu > 0$)

$$\frac{{\rm d}\nu}{{\rm d}\eta} = \frac{6\pi G\hbar}{\alpha^{2/3}}\nu^{4/3}\sin b\cos b, \tag{5.3}$$

$$\frac{{\rm d}b}{{\rm d}\eta} = -\frac{4\pi G\hbar}{\alpha^{2/3}}\nu^{1/3}\sin^2 b, \tag{5.4}$$

$$\frac{{\rm d}A_\gamma}{{\rm d}\eta} = \Pi_\gamma, \qquad \frac{{\rm d}\Pi_\gamma}{{\rm d}\eta} = 0. \tag{5.5}$$

These equations are clearly equivalent to the classical ones in Eq. (2.24) in the classical limit of b being small.

As in the classical theory, Π_γ is a constant of the motion and A_γ increases linearly with respect to the conformal time η. However, the solution for $\nu(\eta)$ is now a hypergeometric function and therefore it is a little harder to see how the quantum corrections modify the classical dynamics.

In order to clarify this point, it is possible to work in proper time $t(N = 1)$—rather than the conformal time used above—as in this case the solution for $\nu(t)$ is much simpler. For $N = 1$, the effective Hamiltonian constraint (already studied in [54]) becomes

$$\mathcal{C}_H^{\rm eff}(t) = -\frac{3\pi G\hbar^2}{2\alpha}\nu\sin^2 b + \frac{3\Pi_\gamma^2}{2(\alpha\nu)^{1/3}} \approx 0, \tag{5.6}$$

and the equations of motion in proper time are

$$\frac{{\rm d}\nu}{{\rm d}t} = \frac{6\pi G\hbar}{\alpha}\nu\sin b\cos b, \tag{5.7}$$

$$\frac{{\rm d}b}{{\rm d}t} = -\frac{3\pi G\hbar}{\alpha}\sin^2 b - \frac{\Pi_\gamma^2}{\hbar\alpha^{1/3}\nu^{4/3}}, \tag{5.8}$$

$$\frac{{\rm d}A_\gamma}{{\rm d}t} = \frac{\Pi_\gamma}{(\alpha\nu)^{1/3}}, \qquad \frac{{\rm d}\Pi_\gamma}{{\rm d}t} = 0. \tag{5.9}$$

Once again, Π_γ is a constant of the motion, but now A_γ is more difficult to solve for. However, this choice makes it much easier to solve for ν. By solving for $\sin^2 b$ via the Hamiltonian constraint, the $\sin b\cos b$ term can be replaced by a function of ν and Π_γ which is easy to integrate as Π_γ is constant. The result is

$$\nu(t) = \frac{1}{\alpha}\left(16\pi G\Pi_\gamma^2(t-t_o)^2 + \frac{3\Pi_\gamma^2}{2\rho_c}\right)^{3/4}, \tag{5.10}$$

where t_o is a constant of integration. Recalling that the scale factor is given by $a = (\alpha\nu)^{1/3}$, this solution shows that for t far away from t_o, the solution approaches the classical trajectory $a(t) \sim \sqrt{|t-t_o|}$, either for a contracting universe ($t < t_o$) or an expanding universe ($t > t_o$). However, there is a major deviation from the classical solution near $t = t_o$ where there is a bounce in the effective solution, providing a bridge between the contracting and expanding classical solutions. This bounce is what allows the effective solution to avoid the classical singularity.

As mentioned above, when using proper time t, it is much harder to solve for $A_\gamma(t)$ (which is a hypergeometric function now), but nonetheless it is possible examine the dynamics of the matter field by looking at the dynamics of the energy density and the pressure, which are still determined by the relations Eqs. (2.16) and (2.17), where $\nu(t)$ is now given by Eq. (5.10).

Note that the bound on the energy density obtained in Eq. (5.2) holds no matter the choice of the time variable. In the case of proper time, it is easy to check that this bound is saturated at $t = t_o$ and that at times far away from t_o, $\rho \ll \rho_c$.

VI. DISCUSSION

In this paper, we tackled the problem of providing a consistent quantization in the LQC framework of a flat FLRW universe filled with radiation. This was achieved by choosing the matter content to be three copies of Maxwell fields as a toy model for a photon gas. For the sake of simplicity, we took the three vector potentials to be homogeneous, orthogonal and to have equal amplitudes—the most straightforward such system that can be coupled to an isotropic geometry.

This particular choice of matter is especially interesting for quantum cosmology as high temperatures are expected in the very early universe, and the basic thermodynamic properties at high temperatures relevant for the cosmology of thermalized matter fields can be modeled by a radiation

gas such as the one studied in this paper. Thus, a radiation-dominated FLRW loop quantum cosmology is of great relevance for the study of the very early universe.

An important difference of these studies with respect to previous works in LQC is that so far the matter content considered in LQC in a genuinely quantum treatment has never actually been a microscopic field observed in nature: the massless scalar field studied in [3] is neither predicted by particle theories nor observed whereas the pressureless dust of [8] is observed only as a large-scale phenomenon, due to the averaged behavior of matter fields over super-galactic scales in cosmology and at micrometer scales in astrophysics. Here by composing the matter content out of Maxwell fields, we have incorporated for the first time in LQC a fundamental matter field that is known to exist.

That being said, it is important to keep in mind that the matter field considered here is not a rigorous simulation of thermal radiation with a large population of fields whose energies follow the Bose-Einstein distribution. Instead, it is a toy model consisting of three orthogonal homogeneous Maxwell vector potentials with equal amplitudes. While this is a particularly nice model due to its simplicity, it is essential to keep in mind the limitations of such a naïve framework.

This system was quantized within the LQC framework following the standard hybrid approach, namely a polymer quantization for geometrical degrees of freedom and the standard Schrödinger quantization for the matter sector. The physical evolution of the quantum system is defined through the set of partial observables parametrized by the amplitude of the vector potential, which plays the role of an internal clock. The resulting dynamics were studied numerically, showing that the quantum dynamics are qualitatively similar to the dynamics for a matter content given by a massless scalar [3] or a pressureless dust field [8]. In addition, sharply peaked semiclassical states remain sharply peaked throughout their evolution, and the global evolution picture features two classical epochs, one each of contraction and expansion—where the dynamics follow to great precision the predictions of general relativity—connected deterministically by the quantum bounce. The matter energy density remains bounded above with the same upper bound found in other contexts, $\rho_c = 3/(8\pi\gamma^2\Delta G)$. Furthermore, again as has been done for other matter fields in LQC, it was possible to define an effective classical description of the system, which accurately mimics the genuine quantum evolution for sharply peaked states. Finally, the scattering picture of the global evolution can be used in order to derive strong triangle inequalities between the dispersions of the wave packet in the distant past and future, which demonstrates the preservation of the semiclassicality of the state across the bounce.

The analytical and numerical findings presented here, together with those of previous works on isotropic LQC, provide a strong indication that the global evolution picture and the preservation of semiclassicality across the bounce are generic features of FLRW universe in LQC: they are independent of the matter content. Thus, the current results are an additional confirmation of the robustness of the main results of LQC reported in the literature.

The model studied here also has a particularly interesting property: the big-bang (or big-crunch) singularity is reached within finite emergent time (this is also the case for a dust-dominated Friedmann cosmology, but not for a massless scalar field). This fact makes it possible to directly address and compare the issue of singularity resolution in LQC and in geometrodynamics for this cosmology. Indeed, for the Wheeler-DeWitt quantization of this system: (i) the singularity is reached within the precision set by the wave packet dispersion, and (ii) the multitude of self-adjoint extensions implies that additional boundary data is needed at the singularity in order to deterministically evolve the wave packet past the point where zero-volume states are reached. These properties amount to the conclusion that in the WDW quantization the singularity is not resolved. This is in stark contrast to the results of the loop quantization, where the unitary evolution is unique and there exists a dynamical minimal volume (proportional to $\langle\Pi_\gamma\rangle^{3/2}G^3\hbar^{9/4}$, which for semi-classical states is much greater than the dispersion of the wave packet). These two results show that the classical singularity is dynamically resolved in LQC.

On the other hand, note that if a positive cosmological constant is added, the low curvature dynamics of the cosmology will be similar to that of the FLRW space-time with a massless scalar field [7]: the vector potential used here as a relational clock will become frozen when the cosmological constant dominates the dynamics, and the infinite volume of the universe will be reached within a finite time. At the quantum level this implies the non-uniqueness of the unitary evolution (i.e., there exist many self-adjoint extensions of the evolution generator), and therefore it is necessary to provide additional data at the boundary $\nu = \infty$ to evolve the wave function beyond this point.

A last important point is that the LQC FLRW cosmology with Maxwell fields is significantly more difficult from a technical standpoint than the case of a massless scalar field. Most notably, the slower rate of convergence of the LQC evolution operator basis elements to their WDW analogs requires an improvement in the numerical techniques involved in the analysis, in particular incorporating higher order LQC corrections to the WDW basis elements. Since this slower convergence is expected to be a feature of generic matter content, the improvement of the numerical treatment that has been presented here is an important further development of LQC.

ACKNOWLEDGMENTS

We would like to thank Jorge Pullin for helpful discussions as well as Brajesh Gupt and Miguel Megevand for the use of their GNUPLOT script to generate

Fig. 1. R. P. would like to thank Carlo Rovelli for his kind hospitality at the Centre de Physique Theorique (CPT). This work was supported in part by Le Fonds québécois de la recherche sur la nature et les technologies, the Spanish MICINN Grant No. FIS2011- 30145-C03-02, the National Center for Science (NCN) of Poland Grants No. 2012/05/E/ST2/03308 and No. 2011/02/A/ST2/00300, the Chilean FONDECYT regular Grant No. 1140335, as well as a grant from the John Templeton Foundation. The opinions expressed in this publication are those of the authors and do not necessarily reflect the views of the John Templeton Foundation. T. P. further acknowledges the financial support of UNAB via internal project DI-562-14/R. The numerical simulations have been performed with the use of the *Numerical LQC* library currently developed by T. Pawłowski, D. Martín-de Blas and J. Olmedo. The developers thank the Department of Mathematics and Statistics of the University of New Brunswick (Canada) for hosting the repository of this library in the period 2011–2013. The bulk of the computations have been performed on the computational cluster "Kruk" at the Institute of Theoretical Physics of Warsaw University (Poland). The figures have been prepared with the use of the GNUPLOT software. The asymptotic expansion of the matrix M_k defined in (B16) was determined with the use of the MATHEMATICA symbolic math software.

APPENDIX A: THE WHEELER-DEWITT ANALOG

In this Appendix we discuss in detail the construction and properties of the WDW quantization of the radiation-dominated FRLW universe—the geometrodynamical analog of the model studied in the main body of the paper. The procedure is as follows: First, in Appendix A 1 we repeat the first two steps of the Dirac program in the context of the WDW quantization, arriving to the dynamics picture, where the evolution is generated by an evolution operator analogous to (3.6). The properties of this operator are next analyzed in Appendix A 2, where all of its self-adjoint extensions are identified. This material provides tools for the analysis of the dynamics of this WDW model presented in Sec. IV A.

1. The Wheeler-DeWitt equation

In a Wheeler-DeWitt quantization, following from geometrodynamics, one quantizes the geometry phase variables using the standard Schrödinger representation rather than the polymer one used in LQC and LQG. The treatment is thus very similar to the standard textbook procedure, although there are some differences due to the cosmological nature of the considered system.

In order to be able to compare the results of this quantization with LQC one should proceed in a way as similar as possible to the latter, in particular by choosing the same variables. However, in order to demonstrate the qualitative properties of the quantum system it is better to start with the original variables $(a, \pi_{(a)})$ used in (2.19).

Before proceeding, we have to note that in standard cosmology a being a scale factor is positive definite. Since geometrodynamics does not involve triads there is no natural reason for equipping it with an orientation. As a consequence the gravitational part of the classical phase space is $\mathbb{R}^+ \times \mathbb{R}$.

This fact has a critical consequence for the quantization. By choosing the lapse $N = a$ (as in LQC) we arrive to the constraint

$$N\mathcal{C}_H = -\frac{\pi G}{3}\pi_{(a)}^2 + \frac{3}{2}\Pi_\gamma^2, \tag{A1}$$

which upon a Schrödigner quantization is equivalent to a *Klein-Gordon equation on a half-line*,[16] with a as the dynamical variable and A_γ time. This system can be described analogously to the Example 2 in Section X.1 of [55]. In this case, the analog of the evolution operator $\underline{\Theta}$ in (3.5) (playing the role of the Hamiltonian) admits a 1-parameter family of self-adjoint extensions, each extension corresponding to different reflective boundary conditions at $a = 0$. We expect similar results when using the variables distinguished by LQC.

Let us now perform the quantization in detail using the same variables and operator ordering choices as in the LQC quantization. We start with the classical phase space now coordinatized by the variables $(\nu, b, A_\gamma, \Pi_\gamma)$ specified in (2.14) and (2.18). The main difference with respect to the treatment above is the fact that now (following LQC where triads play a crucial role) we equip the variable ν with orientation, thus arriving to the classical phase space consisting of two copies of the "purely geometrodynamical" phase space connected at the $\nu = 0$ surface.

By implementing the Schrodinger quantization we arrive to the kinematical Hilbert space of the gravitational sector which is the space of square-integrable functions (the Lebesgue space) with respect to the measure $\mathrm{d}\nu$. As in the case of LQC the parity invariance of the theory allows us to choose the superselection sector of symmetric states $\underline{\Psi}(\nu) = \underline{\Psi}(-\nu)$ and work within this sector only. The variables ν and b are promoted to operators with the action

$$\hat{\nu}\,\underline{\Psi}(\nu) = \nu\underline{\Psi}(\nu), \tag{A2a}$$

$$\hat{b}\,\underline{\Psi}(\nu) = 2i\frac{\partial}{\partial\nu}\underline{\Psi}(\nu). \tag{A2b}$$

We recall that the notation is chosen so that all objects in WDW theory are represented by same symbols as in LQC,

[16] Since the system is a simplification of general relativity that is not well-defined on $a = 0$, one cannot implement any potential barrier there.

although to differentiate them the WDW symbols are underlined.

Replacing the basic variables in the classical Hamiltonian constraint (2.23) by the operators (3.4) and (A2), and choosing a factor-ordering equivalent to the one used in (3.6), gives the Wheeler-DeWitt quantum Hamiltonian constraint,

$$-\frac{\partial^2}{\partial A_\gamma^2}\underline{\Psi}(\nu, A_\gamma) = \underline{\Theta}\,\underline{\Psi}(\nu, A_\gamma), \tag{A3}$$

where the WDW evolution operator is

$$\underline{\Theta} = 18\frac{(2\pi\gamma\sqrt{\Delta}\ell_{\rm Pl}^3)^{1/3}}{\gamma\ell_{\rm Pl}\sqrt{\Delta}\hbar}|\nu|^{1/3}\hat{D}|\nu|^{2/3}\hat{D}|\nu|^{1/3}, \tag{A4}$$

with the operator $\hat{D}$ defined as

$$\hat{D} = \frac{i}{2}\left[\mathrm{sgn}(\nu)\frac{\partial}{\partial\nu} + \frac{\partial}{\partial\nu}\mathrm{sgn}(\nu)\right]. \tag{A5}$$

This particular form of $\hat{D}$ is a consequence of implementing the factor-ordering choices made for the LQC Hamiltonian constraint in this paper (called the sMMO factor-ordering in [43]). On the open domain disjoint from $\nu = 0$, $\underline{\Theta}$ is equivalent to an operator (A4) with $\hat{D}$ replaced with $i\partial_\nu$, however due to presence of $\mathrm{sgn}(\nu)$ special care is required at $\nu = 0$. In particular one has to restrict the domain of $\underline{\Theta}$ [for which one would usually choose the Schwartz space $\mathcal{S}(\mathbb{R})$] setting

$$\mathcal{D}(\underline{\Theta}) = \{\underline{\psi} \in \mathcal{S}(\mathbb{R}) : \underline{\psi}(\nu) = \underline{\psi}(-\nu) \wedge \underline{\psi}(\nu = 0) = 0\}. \tag{A6}$$

From the symmetry and differentiability of $\underline{\psi}$, it follows that

$$\partial_\nu|\nu|^{1/3}\underline{\psi}(\nu)|_{\nu=0} = 0. \tag{A7}$$

The $\underline{\Theta}$ operator is symmetric and non-negative definite on this domain.

Its symmetric eigenfunctions

$$\underline{\Theta}\underline{e}_k(\nu) = \underline{\omega}_k^2\underline{e}_k(\nu) \tag{A8}$$

correspond to positive real eigenvalues, and are Dirac delta normalizable; imposing the normalization to be $\langle\underline{e}_k|\underline{e}_{k'}\rangle = \delta(k - k')$, the eigenfunctions are

$$\underline{e}_k(\nu) = \frac{|\nu|^{-1/3}}{\sqrt{6\pi}}e^{ik|\nu|^{1/3}}, \tag{A9}$$

where the label k (an analog of the wave number) spans the entire real line. The relation between the eigenvalues of $\underline{\Theta}$ and the k labels (the analog of the dispersion relation) is[17]

$$\underline{\omega}_k^2 = 2\frac{(2\pi\gamma\sqrt{\Delta})^{1/3}}{\gamma\sqrt{\Delta}\hbar}k^2. \tag{A10}$$

2. Self-adjoint extensions

It is easy to see by inspection that the Wheeler-DeWitt evolution operator (A4) is symmetric in its domain $\mathcal{D}(\underline{\Theta}) \equiv \mathcal{S}(\mathbb{R})$ and that its spectrum is real and non-negative. However in order to generate unique unitary evolution, the operator has to satisfy the stronger requirement of being essentially self-adjoint. Here we verify this property by studying its deficiency spaces.

The existence and uniqueness of self-adjoint extensions to $\underline{\Theta}$ is particularly important in the context of singularity resolution, as it answers the question whether unitary evolution of the state is possible and whether any additional data is needed at the former classical singularity to determine the evolution uniquely. Once the self-adjoint extensions are known, it is possible to study the dynamics and determine whether the singularity is in fact resolved or not. This is done in Sec. IV A.

Our first step in determining the self-adjoint extension to $\underline{\Theta}$ is the identification of the deficiency subspaces denoted by $\mathcal{K}^\pm$ that are the spaces of normalizable solutions to the equation

$$\underline{\Theta}\underline{e}_{\pm i} = \pm i\underline{e}_{\pm i}, \tag{A11}$$

i.e., normalizable eigenfunctions with eigenvalues $\pm i$. The above equation is easy to solve analytically. Its normalizable solutions are all proportional to the two following normalized functions

$$\underline{e}_{\pm i}(\nu) = \frac{1}{(18\omega_o^2)^{1/4}}\frac{1}{|\nu|^{1/3}}e^{-(1\mp i)|\nu|^{1/3}/\sqrt{2}\omega_o}, \tag{A12}$$

where

$$\omega_o^2 = 2\frac{(2\pi\gamma\sqrt{\Delta})^{1/3}}{\gamma\sqrt{\Delta}\hbar}. \tag{A13}$$

There also exists a second family of formal solutions to (A11) with a growing exponential, but it is not normalizable in the kinematical Hilbert space and therefore it does not contribute to the deficiency space.

As a consequence, each of the deficiency spaces $\mathcal{K}^\pm$ is one-dimensional: $\mathcal{K}^\pm = \mathrm{span}\{\underline{e}_{\pm i}(\nu)\}$. Thus, according to

[17]There is a freedom in the definition of k: we could instead choose $\underline{e}'_k(\nu) = \nu^{-1/3}\sqrt{\ell/6\pi}\exp[i\ell k\nu^{1/3}]$, in which case $(\underline{\omega}')_k^2 = \ell^2\underline{\omega}_k^2$. The (arbitrary) length scale ℓ can clearly be absorbed into the definition of k and this is what is done here.

Theorem X.2 in [55], $\underline{\Theta}$ admits many self-adjoint extensions, each corresponding to a unitary map $U^\alpha\colon K_+ \to K_-$. Since $\dim(\mathcal{K}_+) = \dim(\mathcal{K}_-) = 1$ such maps form a 1-dimensional family parametrized by $\alpha \in [0,\pi)$, each element being $U^\alpha e_+(\nu) = e^{i\alpha} e_-(\nu)$, exactly as expected from the preliminary considerations given in Sec. IV A. Each extended domain $\mathcal{D}_\alpha(\underline{\Theta})$ then takes the form

$$\mathcal{D}_\alpha(\underline{\Theta}) = \{\underline{\psi}_{\rm ext}\colon \underline{\psi}_{\rm ext}(\nu) = \underline{\psi}(\nu) + \lambda \underline{e}_\alpha(\nu), \quad \underline{\psi} \in \mathcal{D}(\underline{\Theta}), \lambda \in \mathbb{C}\}, \tag{A14}$$

where

$$\begin{aligned}\underline{e}_\alpha(\nu) &:= \underline{e}_{+i}(\nu) + e^{i\alpha}\underline{e}_{-i}(\nu)\\ &= \frac{2}{(18\omega_o^2)^{1/4}}\frac{1}{|\nu|^{1/3}} e^{-|\nu|^{1/3}/\sqrt{2}\omega_o}\\ &\quad\times \cos\left(\frac{1}{\sqrt{2}\omega_o}|\nu|^{1/3} - \frac{\alpha}{2}\right) e^{i\frac{\alpha}{2}}.\end{aligned} \tag{A15}$$

Instead of identifying explicit boundary conditions at $\nu = 0$ associated with each extension, in this case it is easier to find the extended bases through the orthogonality requirement. First we note that (A14) and (A15) imply that the basis elements of any self-adjoint extension have to contain balanced "incoming" and "outgoing" components, that is

$$\underline{e}_{\alpha,k} = \frac{1}{\sqrt{3\pi}|\nu|^{1/3}}\cos[k|\nu|^{1/3} + \underline{\varphi}(\alpha,k)]. \tag{A16}$$

The requirement of orthogonality within each extension basis (labeled by α) implies the selection condition

$$\tan[\underline{\varphi}(\alpha,k)] = \frac{\tan[\beta(\alpha)]}{k}, \tag{A17}$$

where $\beta\colon [0,\pi) \to [0,\pi)$ is a bijective function of the extension label α. From now on we will use β as the extension label for technical convenience.

Each self-adjoint extension $\underline{\Theta}_\beta$ of $\underline{\Theta}$ has a nondegenerate spectrum of which the non-negative part (being the only one contributing to the physical sector)[18] is absolutely continuous $\mathrm{Sp}(\underline{\Theta}_\beta) = \mathbb{R}^+\cup\{0\}$. The spaces of physical states (the positive frequency sector) for each extension are

$$\mathcal{H}_\beta \ni \Psi(\nu, A_\gamma) = \int_{\mathbb{R}^+} \mathrm{d}k \tilde{\underline{\Psi}}(k)\underline{e}_{\beta,k}(\nu)e^{i\omega(k)A_\gamma}, \tag{A18}$$

where $\omega(k)$ is given by (A13) and the spectral profile $\tilde{\underline{\Psi}}$ is normalizable in $L^2(\mathbb{R}^+, \mathrm{d}k)$.

[18]Note that due to the non-negativity of $-\partial^2/\partial A_\gamma^2$ on $\mathcal{H}_A$ any *a priori* contribution from the negative part of the spectrum of $\underline{\Theta}_\beta$ would be removed from the physical sector in the process of solving (A3) (equivalently $NC_H = 0$) through group averaging.

APPENDIX B: THE SCATTERING PICTURE

Having at our disposal the well-defined WDW theory of Appendix A, we can relate the asymptotics of the LQC dynamics to the WDW dynamics using the scattering picture introduced in [46]. However, due to the more complicated (as compared to the case of a space-time with a massless scalar field) structure of the WDW theory itself, some improvements have to be made to the method used. In particular, it is necessary to introduce the scattering picture already at the level of the WDW theory itself, using in the process certain auxiliary structures. This is done in Appendix B 1. These structures will be used in Appendix B 2 to build in turn the scattering picture in LQC. Finally, the proper WDW limit of the LQC dynamics is presented in Appendix B 3 and from this it is possible to derive useful triangle inequalities between the dispersions of certain physically interesting observables, as shown in Appendix B 4.

1. Wheeler-DeWitt scattering

As each basis element of a physical Hilbert space has the form of a reflected plane wave, it is natural to split it into the incoming and outgoing components,

$$\underline{e}_{\alpha,k}(\nu) = \frac{1}{\sqrt{2}}(e^{i\underline{\varphi}(\alpha,k)}\underline{e}_k^+ + e^{-i\underline{\varphi}(\alpha,k)}\underline{e}_k^-), \tag{B1}$$

where

$$\underline{e}_k^\pm = \frac{1}{\sqrt{6\pi}|\nu|^{1/3}} e^{\pm ik|\nu|^{1/3}}. \tag{B2}$$

The terms $\underline{e}_k^\pm$ can be thought of as the incoming and outgoing plane waves in the auxiliary Hilbert space $\underline{\mathcal{H}}_{\rm aux}$ constructed by (i) restricting the support of the symmetric wave functions on $\underline{\mathcal{H}}_{\rm phy}$ and (ii) extending it to the (now unphysical) domain $\nu < 0$ by taking the following extension of $\underline{e}_k^\pm$:

$$\tilde{\underline{e}}_k^\pm = \frac{1}{\sqrt{6\pi}|\nu|^{1/3}} e^{\pm ik\,\mathrm{sgn}(\nu)|\nu|^{1/3}}. \tag{B3}$$

Given that, one can treat the reflection of the WDW wave packet at the singularity as a specific example of a scattering, that is the transition

$$\begin{aligned}\int_{\mathbb{R}^+} \mathrm{d}k \tilde{\Psi}_{\rm in}\tilde{\underline{e}}_k^+(\nu)e^{i\omega A_\gamma} &=: \Psi_{\rm in}(\nu, A_\gamma)\\ &\mapsto \Psi_{\rm out}(\nu, A_\gamma) := \int_{\mathbb{R}^+} \mathrm{d}k \tilde{\Psi}_{\rm out}\tilde{\underline{e}}_k^-(\nu)e^{i\omega A_\gamma}.\end{aligned} \tag{B4}$$

The decomposition (B1) implies that

$$e^{-i\underline{\varphi}(\alpha,k)}\tilde{\Psi}_{\rm in}(k) = e^{i\underline{\varphi}(\alpha,k)}\tilde{\Psi}_{\rm out}(k) = \tilde{\Psi}(k), \tag{B5}$$

thus the scattering process is described by the density matrix $\hat{\rho}$, where

$$\rho(k,k') = e^{-2i\underline{\varphi}(\alpha,k)}\delta(k-k'). \tag{B6}$$

The observables $\hat{\underline{\Pi}}_\gamma$ and $\hat{\underline{x}}_{A_\gamma}$ defined on $\underline{\mathcal{H}}_{\rm phy}$ can be transferred in a straightforward way to the observables $\hat{\Pi}_\gamma$ and $\hat{x}_{A_\gamma}$ defined on the auxiliary space $\underline{\mathcal{H}}_{\rm aux}$, such that

$$\hat{\Pi}_\gamma = -\frac{i\hbar}{3}\partial_{A_\gamma}, \qquad \hat{x}_{A_\gamma} = \widehat{\nu^{1/3}_{A_\gamma}}. \tag{B7}$$

Then, for sufficiently localized WDW states, that is states that satisfy $\langle\Delta\hat{\Pi}_\gamma\rangle < \infty$, $\langle\Delta\hat{x}_{A_\gamma}\rangle < \infty$ (see for example [46] for a discussion), we have

$$\lim_{A_\gamma\to\pm\infty}[\langle\underline{\Psi}|\hat{x}_{A_\gamma}|\underline{\Psi}\rangle_{\rm WDW} - \langle\underline{\Psi}_{\rm in/out}|\hat{x}_{A_\gamma}|\underline{\Psi}_{\rm in/out}\rangle_{\rm aux}] = 0, \tag{B8a}$$

$$\lim_{A_\gamma\to\pm\infty}[\langle\underline{\Psi}|\Delta\hat{x}_{A_\gamma}|\underline{\Psi}\rangle_{\rm WDW} - \langle\underline{\Psi}_{\rm in/out}|\Delta\hat{x}_{A_\gamma}|\underline{\Psi}_{\rm in/out}\rangle_{\rm aux}] = 0, \tag{B8b}$$

which allow us to find explicit relations between the dispersions of $\hat{x}_{A_\gamma}$ in the distant future and past. In particular, as the operator $\hat{x}_{A_\gamma}$ on $\underline{\mathcal{H}}_{\rm aux}$ has the form $\hat{x}_{A_\gamma} = -i\partial_k + iA_\gamma[\partial_k\omega]\mathbb{1}$ and the expectation values and dispersions of the operator $-i\partial_k$ on $\underline{\Psi}_{\rm in/out}$ are related via

$$\langle\underline{\Psi}_{\rm out}| - i\partial_k|\underline{\Psi}_{\rm out}\rangle = \langle\underline{\Psi}_{\rm in}| - i\partial_k - 2[\partial_k\underline{\varphi}]\mathbb{1}|\underline{\Psi}_{\rm in}\rangle, \tag{B9a}$$

$$\langle\underline{\Psi}_{\rm out}|\Delta(-i\partial_k)|\underline{\Psi}_{\rm out}\rangle = \langle\underline{\Psi}_{\rm in}|\Delta(-i\partial_k - 2[\partial_k\underline{\varphi}]\mathbb{1})|\underline{\Psi}_{\rm in}\rangle, \tag{B9b}$$

we can easily construct (following the derivation in [46]) a "triangle inequality" involving the dispersions

$$\lim_{A_\gamma\to\infty}\langle\underline{\Psi}|\Delta\hat{x}_{A_\gamma}|\underline{\Psi}\rangle_{\rm WDW} \le \lim_{A_\gamma\to-\infty}\langle\underline{\Psi}|\Delta\hat{x}_{A_\gamma}|\underline{\Psi}\rangle_{\rm WDW} + 2\langle\underline{\Psi}|\Delta(\partial_k\underline{\varphi})|\underline{\Psi}\rangle_{\rm WDW} \tag{B10}$$

where from (A17) it follows that for the self-adjoint extension labeled by β

$$\partial_k\underline{\varphi} = \frac{\tan(\beta)}{k^2+\tan^2(\beta)}\mathbb{1}. \tag{B11}$$

For states sharply peaked in Π_γ the dispersion of the operator $\partial_k\underline{\varphi}$ behaves approximately like $\langle\Delta\partial_k\underline{\varphi}\rangle \sim \langle\Pi_\gamma\rangle^{-3}\langle\Delta\Pi_\gamma\rangle$, thus this inequality shows that there is a strong preservation of semiclassicality in the process of the transition between the "incoming" and "outgoing" modes.

2. LQC scattering

In the case of flat FRLW cosmologies with a massless scalar field, in the large ν limit the eigenfunctions of the LQC evolution operator approach a particular combination of the eigenfunctions of the WDW evolution operator. This permits a description of the global LQC dynamics as the process of a scattering of WDW wave packets in a way similar to the example described in Sec. B 1.

For a radiation-dominated FLRW space-time, a precise analog of this result may not be possible, as each WDW physical Hilbert space element is already a combination of two plane waves. However, the procedure can be generalized so that, instead of using the WDW basis directly, one uses the incoming and outgoing components that form a basis on the auxiliary space defined in (B2).

Therefore, it is necessary to verify the convergence[19] of the basis elements e_k

$$e_k(\nu) = f(k)\underline{e}^+_k(\nu) + f(-k)\underline{e}^-_k(\nu) + |\underline{e}^+_k(\nu)|o(|\nu|^0), \tag{B12}$$

where $|f(k)| = |f(-k)|$ due to the reality of e_k as solutions to (3.13).

The expectation that (B12) holds comes from studying the numerical evaluation of e_k. The convergence to the incoming/outgoing components of the WDW wave packets in the distant past/future has also been observed directly at the level of states. To confirm the validity of (B12), we use the analytic method specified in [56]. Its core elements are:

(1) Rewriting the second order iterative relation between consecutive points of the support of e_k in the first order form

$$\vec{e}_k(\nu+4) = A_k(\nu)\vec{e}_k(\nu), \tag{B13}$$

where

$$\vec{e}_k(\nu) = \begin{pmatrix} e_k(\nu) \\ e_k(\nu-4)\end{pmatrix}, \tag{B14a}$$

$$A_k(\nu) = \begin{pmatrix} \frac{f_o(\nu)-\omega^2(k)}{f_+(\nu)} & -\frac{f_-(\nu)}{f_+(\nu)} \\ 1 & 0\end{pmatrix}, \tag{B14b}$$

with $f_o, f_\pm$ specified via (3.8).

(2) Expressing the values of e_k on each pair of the consecutive points of its support as a linear combination of the WDW components [corresponding to the same $\omega(k)$], which in the notation above can be written as

$$\overrightarrow{e}_k(\nu) = B_k(\nu)\vec{\chi}_k(\nu), \tag{B15a}$$

[19]Here we use the textbook nomenclature where $\lim O(f(x))/f(x) < \infty$ and $\lim o(f(x))/f(x) = 0$.

$$B_k(\nu) = \begin{pmatrix} \underline{e}_k^+(\nu) & \underline{e}_k^-(\nu) \\ \underline{e}_k^+(\nu-4) & \underline{e}_k^-(\nu-4) \end{pmatrix}, \quad \text{(B15b)}$$

where the matrix $B_k(\nu)$ is invertible for sufficiently large $|\nu|$. If the expected convergence (B12) holds, then the coefficient vector χ_k has a well-defined large $|\nu|$ limit.

(3) Rewriting the eigenvalue problem as a first order iterative equation for the coefficient vectors

$$\vec{\chi}_k = M_k(\nu)\vec{\chi}_k, \quad \text{(B16a)}$$

$$M_k(\nu) \coloneqq B_k^{-1}(\nu+4)A(\nu)B_k(\nu). \quad \text{(B16b)}$$

Then the condition sufficient for the convergence (B12) is

$$M_k(\nu) = \mathbb{1} + o(\nu^{-1}), \quad \text{(B17)}$$

and the problem is reduced to probing the asymptotics of $M_k(\nu)$.

Direct inspection shows that

$$M_k(\nu) = \mathbb{1} + O(\nu^{-2}), \quad \text{(B18)}$$

which shows that the relation (B12) indeed holds. Then, the reality of e_k and the comparison of the normalizations in $\mathcal{H}_{\text{phy}}$ and $\mathcal{H}_{\text{aux}}$ (see [43,44,46] for details in an analogous setting) indicate that (B12) can be written as[20]

$$e_k(\nu) = e^{i\varphi(k)}\underline{e}_k^+(\nu) + e^{-i\varphi(k)}\underline{e}_k^-(\nu) + |\underline{e}_k^+(\nu)|O(\nu^{-1}). \quad \text{(B19)}$$

Note that the convergence is one order weaker than for the case of a massless scalar field.

While this result is sufficient to construct the scattering picture, for practical numerical applications (like evaluating $\lim_{\nu\to\infty}\vec{\chi}_k(\nu)$, which is needed for normalization of e_k), the convergence is too slow. The rate of convergence can be improved by replacing the components $\underline{e}_k^\pm$ in (B15) with the functions[21]

$$\underline{e}'_k(\nu) = \frac{|\nu|^{-1/3}}{\sqrt{6\pi}}\left[1 + \frac{k^2}{9|\nu|^{4/3}} + \frac{5k^4}{162|\nu|^{8/3}}\right] \times e^{ik(|\nu|^{1/3} - \frac{2k^2}{81|\nu|} + \frac{4}{27|\nu|^{5/3}} - \frac{2k^4}{945|\nu|^{7/3}})}, \quad \text{(B20)}$$

thus constructing the analog $M_k^{(4)}$ of matrix M_k defined in (B16). Direct inspection of the asymptotics of $M_k^{(4)}$ shows that

$$M_k^{(4)}(\nu) = \mathbb{1} + O(\nu^{-4}), \quad \text{(B21)}$$

which implies that

$$e_k(\nu) = e^{i\varphi(k)}\underline{e}'_k(\nu) + e^{-i\varphi(k)}\underline{e}'_{-k}(\nu) + |\underline{e}'_k(\nu)|O(\nu^{-3}). \quad \text{(B22)}$$

The relation (B19) allows us to again introduce the scattering picture as a mapping of the type (B4) between the auxiliary states, where the spectral profiles of $\underline{\Psi}_{\text{in/out}}$ are related with the LQC spectral profile $\tilde{\Psi}$ (3.16) via

$$e^{-i\varphi(k)}\tilde{\Psi}_{\text{in}}(k) = e^{i\varphi(k)}\tilde{\Psi}_{\text{out}}(k) = \tilde{\Psi}(k), \quad \text{(B23)}$$

which gives a scattering matrix of the form

$$\rho(k,k') = e^{-2i\varphi(k)}\delta(k-k'). \quad \text{(B24)}$$

Due to the oscillatory nature of the first subleading correction in (B19), it is possible to relate the distant past/future expectation values and observables for localized LQC states (defined by the conditions $\langle\Delta\hat{\Pi}_\gamma\rangle < \infty$ and $\langle\Delta\hat{x}_{A_\gamma}\rangle < \infty$) with those of the incoming/outgoing auxiliary states

$$\lim_{A_\gamma\to\pm\infty}[\langle\Psi|\hat{x}_{A_\gamma}|\Psi\rangle - \langle\underline{\Psi}_{\text{in/out}}|\hat{x}_{A_\gamma}|\underline{\Psi}_{\text{in/out}}\rangle_{\text{aux}}] = 0, \quad \text{(B25a)}$$

$$\lim_{A_\gamma\to\pm\infty}[\langle\Psi|\Delta\hat{x}_{A_\gamma}|\Psi\rangle - \langle\underline{\Psi}_{\text{in/out}}|\Delta\hat{x}_{A_\gamma}|\underline{\Psi}_{\text{in/out}}\rangle_{\text{aux}}] = 0, \quad \text{(B25b)}$$

by adapting the construction given in Appendix A2 of [46] to this setting.

3. The WDW limit of LQC dynamics

Because the basis $\underline{e}_k$ of the WDW quantum cosmology is slightly more complicated than in the case of the massless scalar field, it was necessary to define the scattering of the LQC states by using the auxiliary space and its basis functions. In consequence, the results given in Sec. B 2 do not provide a direct relation between the LQC and WDW states.

Fortunately, it is possible (and easy) to describe the evolution of the WDW state itself as the scattering of the

[20] At this point it is not yet obvious if we can relate the normalization of e_k on $\mathcal{H}_{\text{phy}}$ with the normalization of $e^{i\varphi(k)}\underline{e}_k^+(\nu) + e^{-i\varphi(k)}\underline{e}_k^-(\nu)$ on $\mathcal{H}_{\text{aux}}$ that was derived in [46] for second order convergence. However, we see from (B20) that the first subleading term is oscillatory, so the decay rate of ν^{-1} is indeed sufficient for it to not contribute to the normalization.

[21] A systematic procedure to determine this function is to calculate the subleading terms order by order by using the constraints that arise from imposing the appropriate level of convergence on the analog $M_k^{(l)}$ of M_k corresponding to given order l.

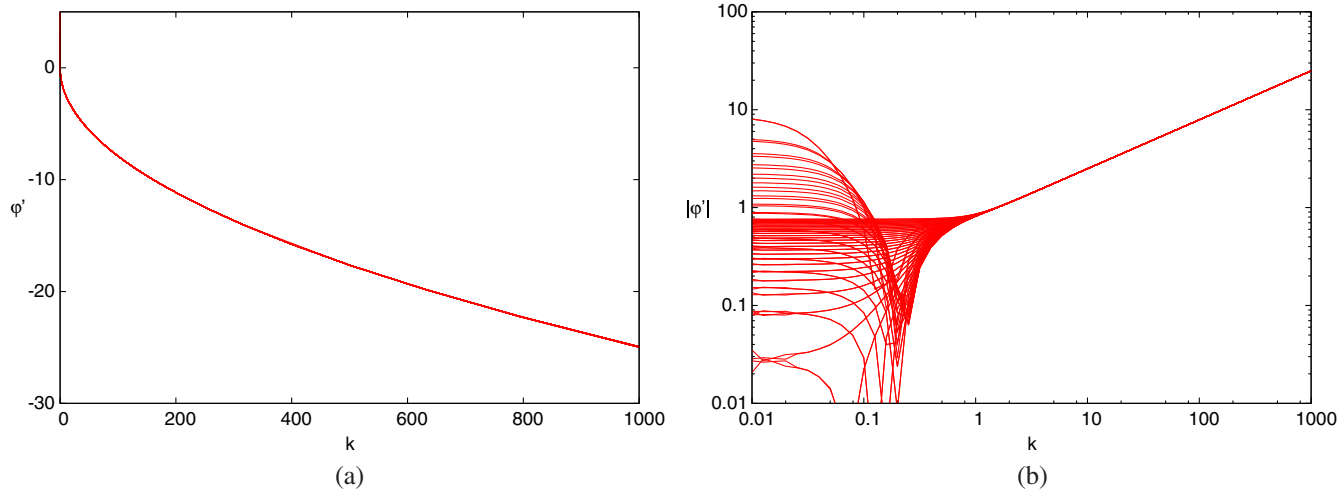

FIG. 3 (color online). The behavior of $\varphi'(k) = \partial_k \varphi(k)$ as a function of k is presented for generic superselection sectors (without differentiating between branches corresponding to different values of ϵ). (a) presents its behavior in linear scale, whereas (b) shows its absolute value in logarithmic scale.

auxiliary state. Furthermore, the auxiliary space emerging in the scattering picture of LQC state is the same as for WDW. This allows us to employ the auxiliary in/out states as an intermediate providing the relation between the LQC and WDW states. Indeed, given an LQC state, the WDW *in* (*out*) state is defined by the requirement that the auxiliary *in* (*out*) component in the scattering description of that state agrees with the auxiliary *in* (*out*) component in the scattering description of the LQC state itself.

In other words, the relation between the spectral profiles of these states—given by (B5) and (B23)—takes the form

$$e^{i[\underline{\varphi}(\alpha,k)-\varphi(k)]}\tilde{\underline{\Psi}}_{\text{in}} = e^{-i[\underline{\varphi}(\alpha,k)-\varphi(k)]}\tilde{\underline{\Psi}}_{\text{out}} = \tilde{\Psi}(k), \tag{B26}$$

where $\alpha'(\alpha, k)$ is given by (A17) and $\tilde{\underline{\Psi}}_{\text{in}}$ and $\tilde{\underline{\Psi}}_{\text{out}}$ are the spectral profiles of the WDW in and out states respectively. As a consequence, we can describe the global LQC evolution as the *scattering of WDW states*. The scattering matrix of this process is given by

$$\rho(k, k') = e^{-2i[\varphi(k)-\underline{\varphi}(\alpha,k)]}\delta(k - k'). \tag{B27}$$

It is important to remember that defining this picture requires us to choose one particular (labeled by α) self-adjoint extension of $\underline{\Theta}$. The scattering matrix (B27) depends on this choice.

The relations (B8) and (B25) allow us to provide a relation between the expectation values and dispersions of the $\hat{x}_{A_\gamma}$ operator in the distant future and past,

$$\lim_{A_\gamma \to \pm\infty} [\langle \Psi|\hat{x}_{A_\gamma}|\Psi\rangle - \langle \underline{\Psi}_{\text{in/out}}|\hat{x}_{A_\gamma}|\underline{\Psi}_{\text{in/out}}\rangle_{\text{WDW}}] = 0, \tag{B28a}$$

$$\lim_{A_\gamma \to \pm\infty} [\langle \Psi|\Delta\hat{x}_{A_\gamma}|\Psi\rangle - \langle \underline{\Psi}_{\text{in/out}}|\Delta\hat{x}_{A_\gamma}|\underline{\Psi}_{\text{in/out}}\rangle_{\text{WDW}}] = 0. \tag{B28b}$$

The expectation values and dispersion of the operator $\hat{\Pi}_\gamma$ of the in/out WDW states are exactly that of the LQC state, since the relations (B5) and (B23) are only phase rotations.

4. The triangle inequality

While in Sec. B 3 we defined a precise description of the global evolution of the LQC state as the scattering of certain WDW states, to relate the spreads of the LQC state in the distant future and past we will employ the scattering picture defined in Sec. B 2 which uses the auxiliary states. This choice is motivated by the fact that in the auxiliary space the operator $\hat{x}_{A_\gamma}$ has a simple analytical form in the k-representation. Indeed, the kinematical operator (or the physical observable in the deparametrization picture) is

$$\hat{x} = -i\partial_k + [\partial_k \omega]A_\gamma \mathbb{1}. \tag{B29}$$

That, together with (B25), allows us to immediately write down the triangle inequality analogous to (B10),

$$\lim_{A_\gamma \to \infty} \langle \Psi|\Delta\hat{x}_{A_\gamma}|\Psi\rangle \le \lim_{A_\gamma \to -\infty} \langle \Psi|\Delta\hat{x}_{A_\gamma}|\Psi\rangle + 2\langle \Psi|\Delta[\partial_k \varphi(k)]|\Psi\rangle. \tag{B30}$$

Unlike in the WDW case however, now we cannot determine $\partial_k \varphi(k)$ analytically. In order to obtain a useful inequality we need to analyze the bounds on $\partial_k \varphi(k)$ numerically. For that we implement the exact method used originally in [46] based on numerically probing the asymptotics of the function $\partial_k e_k(\nu)$. The only difference is that here, instead of using the original auxiliary basis elements (B2), we use the corrected ones (B20), which

provide faster convergence and higher precision. The results are presented on Fig. 3. We see an explicit convergence (at large k) to the function

$$\partial_k \varphi(k) = A\sqrt{k} + o(1), \tag{B31}$$

where the constant A has been determined numerically to equal $A = -0.789 \pm 0.005$.

The exact behavior of $\partial_k \varphi(k)$ depends on the superselection sector labeled by ϵ. Let us start with the sector $\epsilon = 0$. In that case, one of important observations following from numerical studies is the property that

$$|\sqrt{k}\partial_k^2 \varphi(k)| \leq A/2, \tag{B32}$$

which allows us to conclude (via a derivation analogous to that of Sec. 5A in [46])

$$\langle \Psi | \Delta \partial_k \varphi | \Psi \rangle \leq \frac{A}{2} \langle \Psi | \Delta \sqrt{k} | \Psi \rangle. \tag{B33}$$

As a consequence the triangle inequality (B30) implies the following one,

$$\lim_{A_\gamma \to \infty} \langle \Psi | \Delta \hat{x}_{A_\gamma} | \Psi \rangle \leq \lim_{A_\gamma \to -\infty} \langle \Psi | \Delta \hat{x}_{A_\gamma} | \Psi \rangle + A \langle \Psi | \Delta \sqrt{k} | \Psi \rangle, \tag{B34}$$

which only involves observables with a clear physical interpretation as the observable $\sqrt{k}$ can be easily replaced by the Dirac observable $\sqrt{\Pi_\gamma}$.

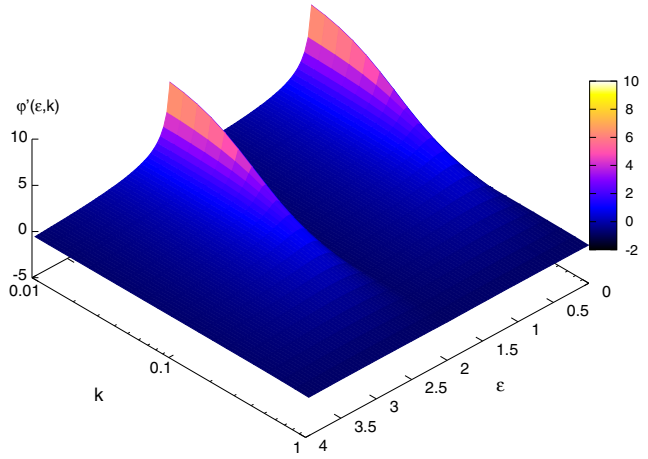

FIG. 4 (color online). The behavior of $\varphi' = \partial_k \varphi$ as a function of both k and the superselection sector label ϵ is shown for small k.

In the case of generic ϵ the situation is slightly more involved, as the numerical studies show significant differences in the behavior of $\partial_k \varphi(k)$ for small values of k. We observe the right-hand discontinuity at $\epsilon = 0$ and $\epsilon = 2$. The bound (B32), while preserved for $k > k_\star \approx 0.15$ may be violated for $k < k_\star$. The exact behavior of $\partial_k \varphi$ as the function of both ϵ and k is presented on Fig. 4. As a consequence, for generic ϵ the triangle inequality (B34) is ensured to hold strictly only for the states whose support does not overlap with the set $k \in [0, k_\star]$.

[1] A. Ashtekar and P. Singh, Classical Quantum Gravity **28**, 213001 (2011); K. Banerjee, G. Calcagni, and M. Martín-Benito, SIGMA **8**, 016 (2012); I. Agullo and A. Corichi, arXiv:1302.3833; M. Bojowald, Living Rev. Relativity **11**, 4 (2008).

[2] M. Bojowald, Phys. Rev. Lett. **86**, 5227 (2001).

[3] A. Ashtekar, T. Pawłowski, and P. Singh, Phys. Rev. D **74**, 084003 (2006).

[4] A. Ashtekar, A. Corichi, and P. Singh, Phys. Rev. D **77**, 024046 (2008).

[5] A. Ashtekar, T. Pawłowski, P. Singh, and K. Vandersloot, Phys. Rev. D **75**, 024035 (2007).

[6] Ł. Szulc, W. Kamiński, and J. Lewandowski, Classical Quantum Gravity **24**, 2621 (2007); K. Vandersloot, Phys. Rev. D **75**, 023523 (2007); Ł. Szulc, Classical Quantum Gravity **24**, 6191 (2007).

[7] E. Bentivegna and T. Pawłowski, Phys. Rev. D **77**, 124025 (2008); T. Pawłowski and A. Ashtekar, Phys. Rev. D **85**, 064001 (2012).

[8] V. Husain and T. Pawłowski, Classical Quantum Gravity **28**, 225014 (2011).

[9] V. Husain and T. Pawlowski, Phys. Rev. Lett. **108**, 141301 (2012).

[10] J. Świeżewski, Classical Quantum Gravity **30**, 237001 (2013).

[11] A. Ashtekar and E. Wilson-Ewing, Phys. Rev. D **79**, 083535 (2009).

[12] M. Martín-Benito, L. J. Garay, G. A. Mena Marugán, and E. Wilson-Ewing, J. Phys. Conf. Ser. **360**, 012031 (2012).

[13] A. Ashtekar and E. Wilson-Ewing, Phys. Rev. D **80**, 123532 (2009); E. Wilson-Ewing, Phys. Rev. D **82**, 043508 (2010); P. Singh and E. Wilson-Ewing, Classical Quantum Gravity **31**, 035010 (2014).

[14] L. J. Garay, M. Martín-Benito, and G. A. Mena Marugán, Phys. Rev. D **82**, 044048 (2010); M. Martín-Benito, G. A. Mena Marugán, and E. Wilson-Ewing, Phys. Rev. D **82**, 084012 (2010).

[15] M. Martín-Benito, D. Martín-de Blas, and G. A. Mena Marugán, Phys. Rev. D **83**, 084050 (2011).

[16] B. Gupt and P. Singh, Phys. Rev. D **86**, 024034 (2012).

[17] D. Brizuela, G. A. Mena Marugan, and T. Pawlowski, Classical Quantum Gravity **27**, 052001 (2010); Phys. Rev. D **84**, 124017 (2011).

[18] M. Bojowald, G. M. Hossain, M. Kagan, and S. Shankaranarayanan, Phys. Rev. D **79**, 043505 (2009); E. Wilson-Ewing, Classical Quantum Gravity **29**, 085005 (2012); T. Cailleteau, J. Mielczarek, A. Barrau, and J. Grain, Classical Quantum Gravity **29**, 095010 (2012).

[19] M. Fernandez-Mendez, G. A. Mena Marugán, and J. Olmedo, Phys. Rev. D **86**, 024003 (2012); I. Agullo, A. Ashtekar, and W. Nelson, Phys. Rev. D **87**, 043507 (2013).

[20] A. Dapor, J. Lewandowski, and J. Puchta, Phys. Rev. D **87**, 104038 (2013).

[21] E. Wilson-Ewing, Classical Quantum Gravity **29**, 215013 (2012).

[22] M. Bojowald, G. Calcagni, and S. Tsujikawa, J. Cosmol. Astropart. Phys. 11 (2011) 046; L. Linsefors, T. Cailleteau, A. Barrau, and J. Grain, Phys. Rev. D **87**, 107503 (2013); I. Agullo, A. Ashtekar, and W. Nelson, Classical Quantum Gravity **30**, 085014 (2013).

[23] E. Wilson-Ewing, J. Cosmol. Astropart. Phys. 03 (2013) 026; Y.-F. Cai and E. Wilson-Ewing, J. Cosmol. Astropart. Phys. 03 (2014) 026.

[24] E. Wilson-Ewing, J. Cosmol. Astropart. Phys. 08 (2013) 015.

[25] J. Lewandowski, M. Domagala, and M. Dziendzikowski, *Proc. Sci.*, QGQGS2011 (2011) 025; M. Domagala, M. Dziendzikowski, and J. Lewandowski, arXiv:1210.0849.

[26] A. Kreienbuehl and T. Pawłowski, Phys. Rev. D **88**, 043504 (2013).

[27] S. S. Seahra, I. A. Brown, G. M. Hossain, and V. Husain, J. Cosmol. Astropart. Phys. 10 (2012) 041.

[28] A. Ashtekar, T. Pawłowski, and P. Singh (to be published).

[29] M. Artymowski and Z. Lalak, J. Cosmol. Astropart. Phys. 09 (2011) 017.

[30] C. Rovelli, Phys. Rev. D **65**, 124013 (2002); B. Dittrich, Classical Quantum Gravity **23**, 6155 (2006).

[31] A. Golovnev, V. Mukhanov, and V. Vanchurin, J. Cosmol. Astropart. Phys. 06 (2008) 009; C. Armendariz-Picon, J. Cosmol. Astropart. Phys. 07 (2004) 007.

[32] C. W. Misner, K. S. Thorne, and J. A. Wheeler, *Gravitation* (W.H. Freeman and Company, San Francisco, 1973), Sec. 22.5.

[33] A. Ashtekar, M. Bojowald, and J. Lewandowski, Adv. Theor. Math. Phys. **7**, 233 (2003).

[34] A. Corichi and P. Singh, Phys. Rev. D **78**, 024034 (2008); **80**, 044024 (2009).

[35] A. Corichi and E. Montoya, Int. J. Mod. Phys. D **21**, 1250076 (2012); Phys. Rev. D **84**, 044021 (2011).

[36] V. Lapchinsky and V. Rubakov, Teor. Mat. Fiz. **33**, 364 (1977).

[37] J. F. Barbero G., Phys. Rev. D **51**, 5507 (1995).

[38] A. Ashtekar and J. Lewandowski, Classical Quantum Gravity **14**, A55 (1997).

[39] C. Rovelli and E. Wilson-Ewing, Phys. Rev. D **90**, 023538 (2014).

[40] A. Ashtekar, T. Pawłowski, and P. Singh, Phys. Rev. Lett. **96**, 141301 (2006).

[41] T. Thiemann, Classical Quantum Gravity **15**, 839 (1998).

[42] M. Martín-Benito, G. A. Mena Marugán, and J. Olmedo, Phys. Rev. D **80**, 104015 (2009).

[43] G. A. Mena Marugán, J. Olmedo, and T. Pawłowski, Phys. Rev. D **84**, 064012 (2011).

[44] A. Ashtekar, T. Pawłowski, and P. Singh, Phys. Rev. D **73**, 124038 (2006).

[45] J. F. Barbero G., T. Pawłowski, and E. J. S. Villaseñor, Phys. Rev. D **90**, 067505 (2014).

[46] W. Kamiński and T. Pawłowski, Phys. Rev. D **81**, 084027 (2010).

[47] W. Kamiński and J. Lewandowski, Classical Quantum Gravity **25**, 035001 (2008).

[48] A. Ashtekar, J. Lewandowski, D. Marolf, J. Mourão, and T. Thiemann, J. Math. Phys. (N.Y.) **36**, 6456 (1995); D. Marolf, arXiv:gr-qc/9508015; Classical Quantum Gravity **12**, 1199 (1995); **12**, 1441 (1995); **12**, 2469 (1995).

[49] W. Kamiński, J. Lewandowski, and T. Pawłowski, Classical Quantum Gravity **26**, 245016 (2009).

[50] W. Kamiński, J. Lewandowski, and T. Pawłowski, Classical Quantum Gravity **26**, 035012 (2009).

[51] M. Domagala and J. Lewandowski, Classical Quantum Gravity **21**, 5233 (2004).

[52] A. Dapor, W. Kamiński, J. Lewandowski, and J. Świeżewski, Phys. Rev. D **88**, 084007 (2013).

[53] V. Taveras, Phys. Rev. D **78**, 064072 (2008); P. Singh and K. Vandersloot, Phys. Rev. D **72**, 084004 (2005).

[54] A. Ashtekar and E. Wilson-Ewing, Phys. Rev. D **78**, 064047 (2008).

[55] M. Reed and B. Simon, *Methods of Modern Mathematical Physics. 2. Fourier Analysis, Selfadjointness* (Academic Press, New York, 1975).

[56] W. Kamiński and T. Pawłowski, Phys. Rev. D **81**, 024014 (2010).